

ENVIRONMENTAL MICROBIOLOGY
AS RELATED TO PLANETARY QUARANTINE

Semiannual Progress Report 14
June 1975

Supported by
NASA Grant NGL 24-005-160

Submitted to the
National Aeronautics and Space Administration
Washington, D.C.

by


Division of Environmental Health
School of Public Health in association with the
Space Science Center at the University of Minnesota

Contributors:

Donald Fisher
Rebecca Gove
Yvonne Heisserer

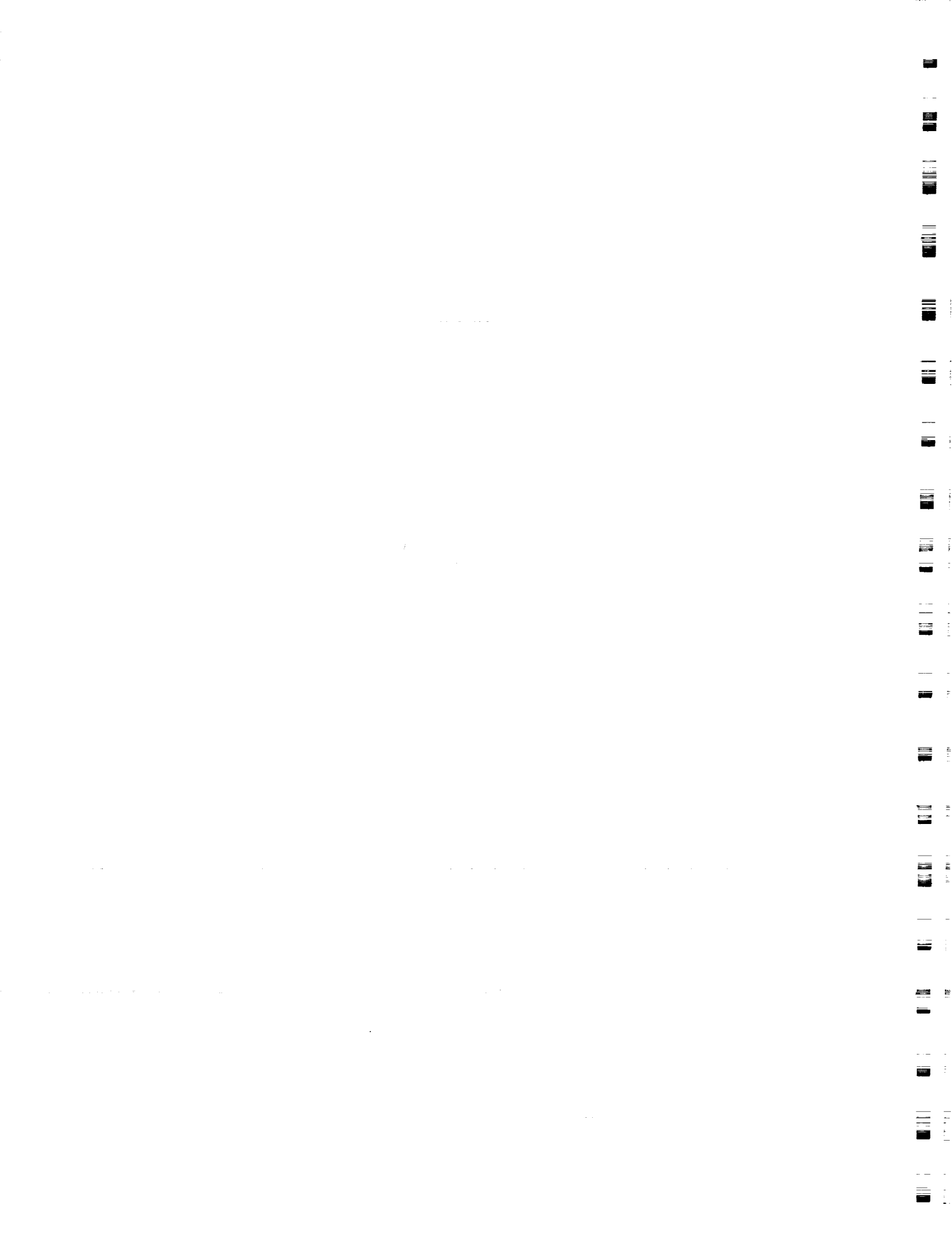
Ron Jacobson
Nancy Kasner
I. J. Pflug

Geraldine Smith
Steven Znameroski



Professor
Project Leader

543 Space Science Center
University of Minnesota
Minneapolis, Minnesota 55455



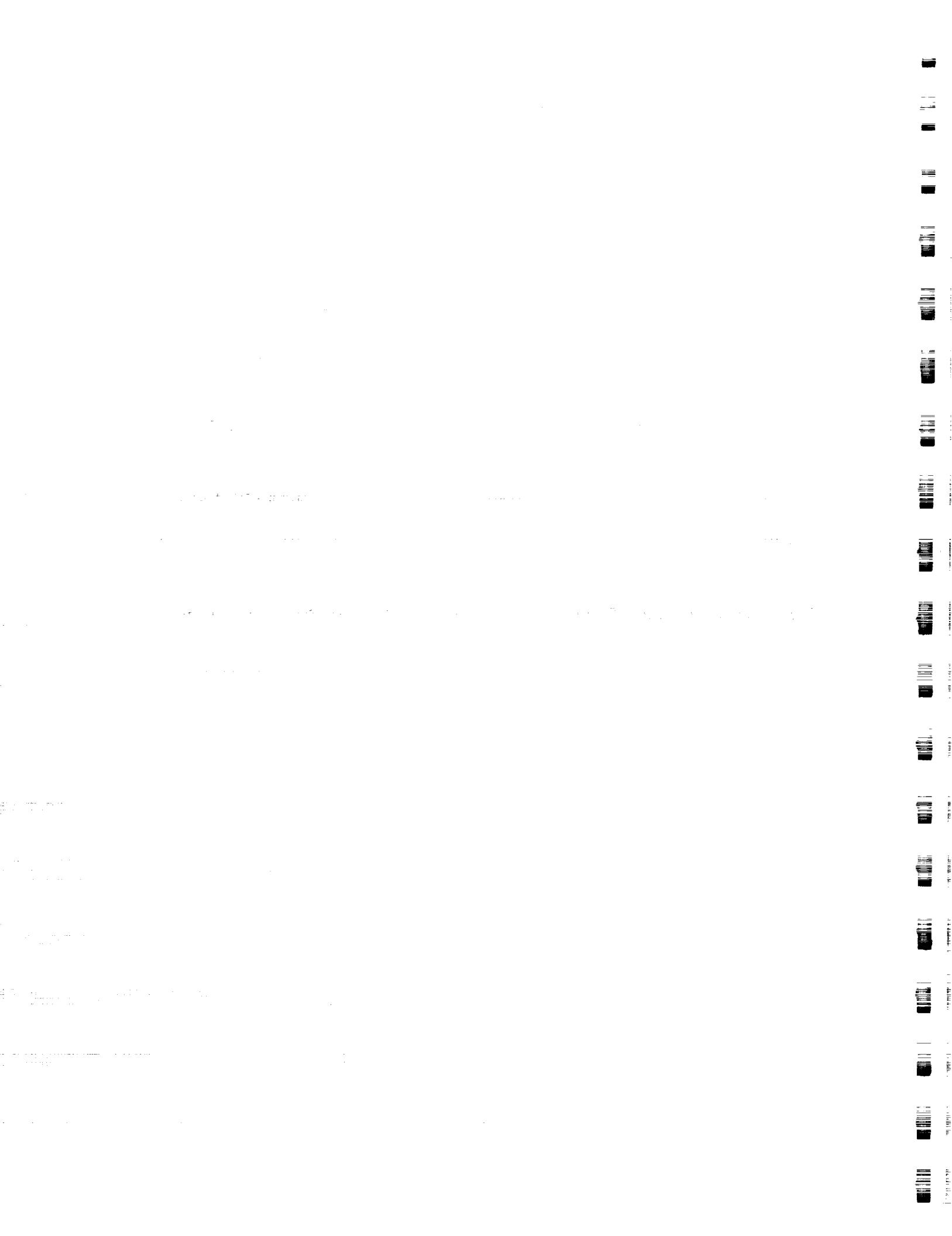
INTRODUCTION

This is the concluding report on the study to further evaluate the effect of combined heat and radiation on microbial destruction.

This work was carried out under NASA Grant NGL 24-005-160. Dr. Lawrence B. Hall of NASA and Richard G. Bond of the University of Minnesota were instrumental in seeing that this work was carried out.

A direct result of this study is additional knowledge regarding microbial destruction by combined heat and radiation.

Dry-heat thermoradiation experiments show a synergistic effect, the degree of which depends on radiation intensity, temperature, and relative humidity. A physical and mathematical model has been derived which first of all predicts a synergistic effect, and secondly displays a priori many of the salient features experimentally observed. This model is useful for the execution of further thermoradiation experiments and relates to future testing for synergistic effects between other combinations of physical stresses.



1. EFFECT OF COMBINED HEAT AND RADIATION ON MICROBIAL DESTRUCTION

Donald A. Fisher and Irving J. Pflug

INTRODUCTION

This is the concluding report of a study of the effect of combined heat and radiation on microbial destruction that was begun in June, 1971. The development of the environmental system that was used in the thermal radiation study is described in Progress Report numbers 7 and 8. In Progress Report number 9 the results of studies of combined wet heat and radiation are reported.

Interest in thermal radiation in the past has been primarily directed toward combined dry heat and radiation; however, in this study we have evaluated both dry heat and wet heat combined with gamma radiation.

In carrying out this project we have attempted to not only develop destruction rate data but to also determine the mechanistic basis for the synergism that results when microorganisms are subjected to these two seemingly independent lethal agents.

OBJECTIVES

The objectives of this project were: (1) to investigate the synergistic effect which results when bacterial spores are subjected to simultaneous heat and gamma radiation, thereby enabling us to

specify thermoradiation cycles, and (2) to derive a clearer understanding of the underlying mechanism which leads to non-viability of bacterial spores.

MATERIALS AND METHODS

To study the combined effect of dry heat and gamma radiation, bacterial spores were deposited from an alcohol suspension onto stainless steel planchets. The inoculated planchets were then subjected to heat and radiation treatments in an environmental system located at the Gamma Radiation Facility of the University of Minnesota. Details of each step of the experimental protocol are outlined below.

Exposure Chamber

The environmental chamber shown in Figure 1.1 was a modular unit of the Thermoradiation Environmental System (TRES) described in Progress Reports number 7, 8 and 9. Using sterile forceps the inoculated planchets were placed in one of three holders in the chamber so the inoculated side of the planchet would be facing the gamma source. They were clamped in place by thin edges. The holders were mounted on rails in the chamber and could be moved along the track to positions previously determined to be the points at which the desired radiation intensity occurred (see section which describes dosimetry). Duplicate planchets were placed in each holder. Two thermocouples were located in the environment of the chamber and were used to monitor the treatment temperature. A photograph showing the sample holder and one planchet and a thermocouple is shown in Figure 1.2.

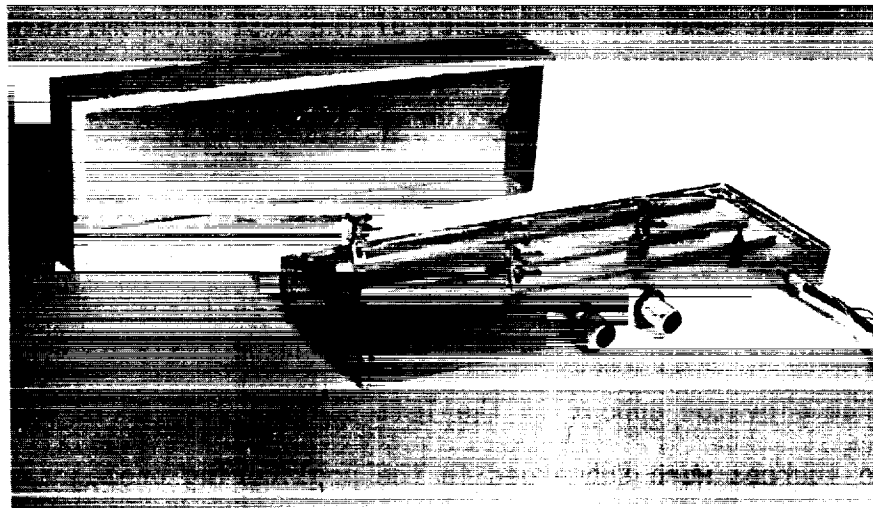


Figure 1.1: Environmental chambers used in dry heat thermoradiation



Figure 1.2: Sample holder in environmental chamber

Test System Arrangement

To increase the efficiency of the test program, several psychrometric conditions were tested concurrently. This was achieved by using five separate environmental chambers each with an airstream being drawn from one of two saturation chambers. The five environmental chambers were placed compactly with ray symmetry around the radiation source elevator as shown in Figure 1.3. The guide rails of the radiation source elevator appear in the left central portion of the photograph (the sources were submerged in the pool during photography for obvious safety reasons). The spray chambers used to control the saturation temperature are on the right, with the blowers and wet and dry bulb assemblies located between the spray chambers and environmental chambers.

Radiation Dosimetry

The Cesium-137 radiation sources have been described in Progress Report number 7. The dose rate profile within each environmental chamber was measured by locating bottles of Fricke solution at the points normally occupied by the biological samples. After radiation for a known period of time, the solutions were analyzed to determine the radiation intensities at the respective sites. The location of the holders were adjustable so the samples would receive the desired radiation intensity. Radiation dose rates of 20, 10, and 5 Krd/hr (water) were used in these studies.



Figure 1.3: Composite heating system in Gamma Irradiation Facility

Heated Non-Radiated Testing

Studies to measure the effect of heat without radiation on microbial spore destruction were carried out using the same apparatus, however it was assembled and operated outside the Gamma Radiation Facility. The same remote control operation of the system was used during testing outside the facility so the thermal conditions that the spore samples experienced when tests were performed inside the facility were duplicated.

Sequence of Operations for Testing

All experiments were performed with the same general operation method:

1. First the temperatures of the spray reservoirs were regulated to the desired saturation temperature.
2. The testing apparatus was assembled in the Gamma Radiation Facility, with extreme care given to the precise positioning of the environmental chambers each time. A template was used to ensure high precision in repeated positioning of the chambers relative to the source elevator.
3. The system was heated and the proportional controllers were set to the temperatures needed for biological testing.
4. With the heaters in the environmental chamber off, the chambers were opened and inoculated planchets were clamped in their test positions. The chambers were once again closed and clamped shut, placed in insulated styrofoam boxes, and secured in position. The heaters were again activated, and the chambers were heated to the

test temperature. During this heating operation, ambient air was drawn through the chamber so that the relative humidity during this period was much lower than would be encountered subsequently during the treatment period. Over the range of temperatures investigated, the low relative humidities encountered during the heat-up period were considered to produce non-lethal conditions.

5. Once test temperatures were reached, connections to the spray chamber were made and the pre-heater (which heated the air stream above the saturation temperature upon leaving the saturation chamber) was turned on.
6. The system was set to run.
7. The spray pump was turned on producing a step jump in the humidity level in the environmental chamber and therefore a step in the lethal conditions as well. The Gamma Facility was then secured and personnel safety precautions were taken. The elevator carrying the source configuration was raised to its operating position at which time treatment was considered to have started. The time delay from starting of the spray pumps until final positioning of the sources was approximately 40 seconds.
8. During the treatment period, the temperatures at various points within the system were monitored. A Honeywell Model 15 recording potentiometer measured the outputs from the thermocouples. The operator adjusted the proportional controllers as needed to maintain the experiment within control limits.

9. At the end of the treatment period, the Cesium source was submerged into the facility pool, personnel safety precautions were completed, the Gamma Facility was opened, the spray pump was stopped, and the hoses were disconnected from the spray chamber.
10. Ambient air was then circulated through the chambers for approximately two minutes with the chamber heaters still turned on. The procedure prevented water condensation on the inoculated surfaces.
11. The heaters were then turned off, the environmental chambers were reopened, planchets removed and placed in sterile flasks, and another set of untreated samples were placed in holders. Aseptic technique was used in handling, placement, and removal of planchets.
12. The system was set for the entire procedures to be repeated for the next treatment period.

Treatment periods were successive to one another, the sequence of which was chosen in a random fashion.

Bacteriological Procedures

The group of spores used in this portion of the study, Bacillus subtilis var. niger (AAHK), were taken from the same spore crop as the spores used in the wet heat tests described in Progress Report #9 (AAHF) except that they had been suspended and stored in alcohol (instead of water) since July, 1972.

These spores (AAHK) were deposited on a 1/2" x 1/2" stainless steel planchet from 10 ml of an alcohol suspension using an Eppendorf micropipette. Each planchet deposit had a spore population of 2.5×10^6 . The planchets had been thoroughly cleaned and oven sterilized.

The inoculated planchets were allowed to equilibrate overnight in the clean room environment (22°C, 50% RH) after which they were placed in a sterile petri dish and carried to the Gamma Facility for testing.

During manipulation of samples in the Gamma Facility, sterile transfer procedures were followed. Even though the Gamma Facility is not a biologically clean area, no contamination problems were encountered, no doubt due in part to the self-sterilizing ability of the facility.

After treatment, the planchets were placed in sterile flasks and returned to the clean room for processing according to NASA standard procedures.

Conditions Tested

Tests were run at a number of psychrometric conditions. These conditions are shown in Figure 1.4 and cover most of the range of controllable lethal conditions that the thermoradiation environmental system was capable of producing. Replicate experiments were performed at each condition in order to give better confidence in the results.

RESULTS

Survivor curves are presented in Figures 1.5 through 1.17 for all of the conditions which were investigated. In all cases, results are presented on the same graph for radiation intensities of 20, 10 and 5 Krd/hr at a common psychrometric condition. In most cases, results are

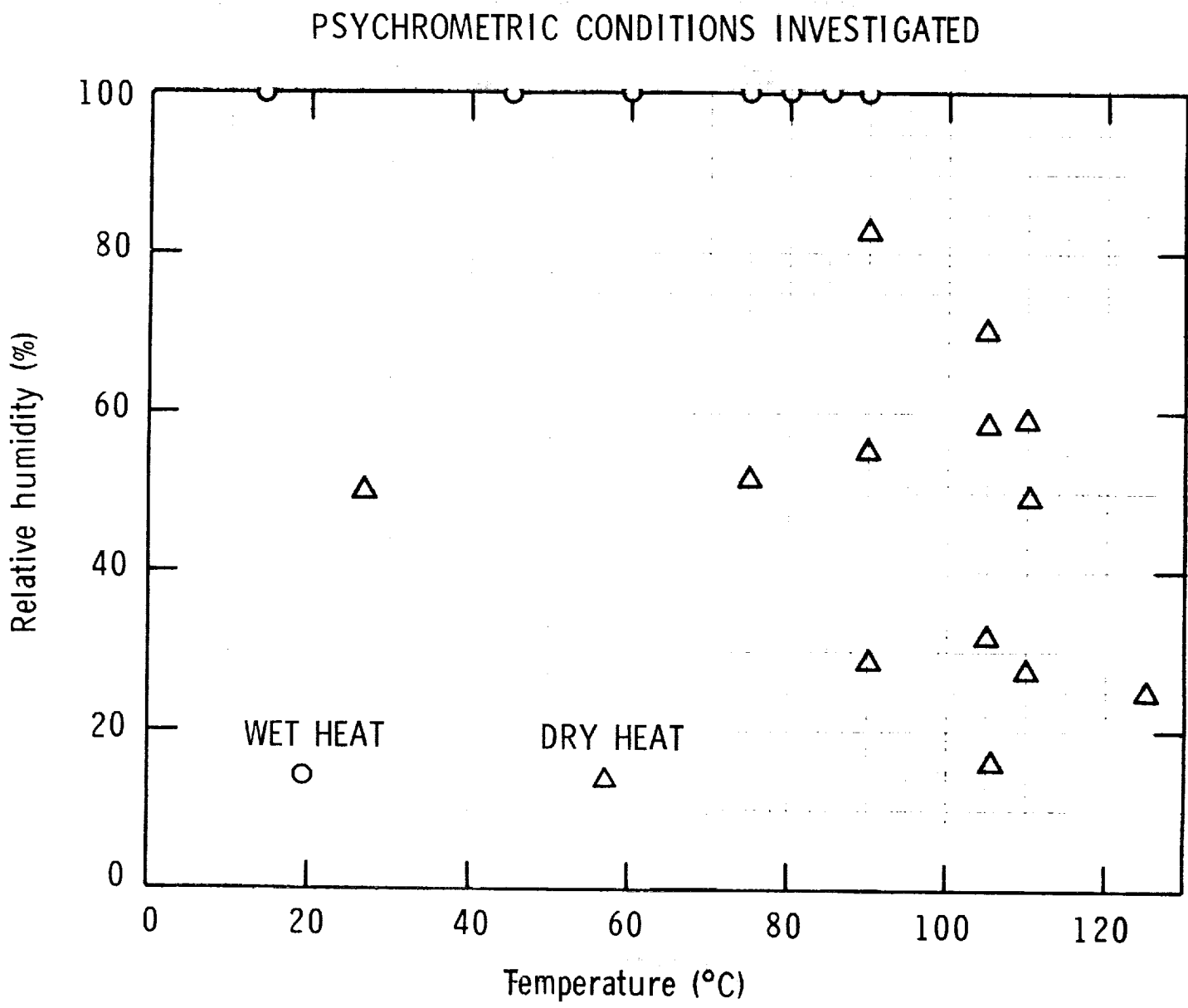


Figure 1.4: Psychrometric conditions examined in this study

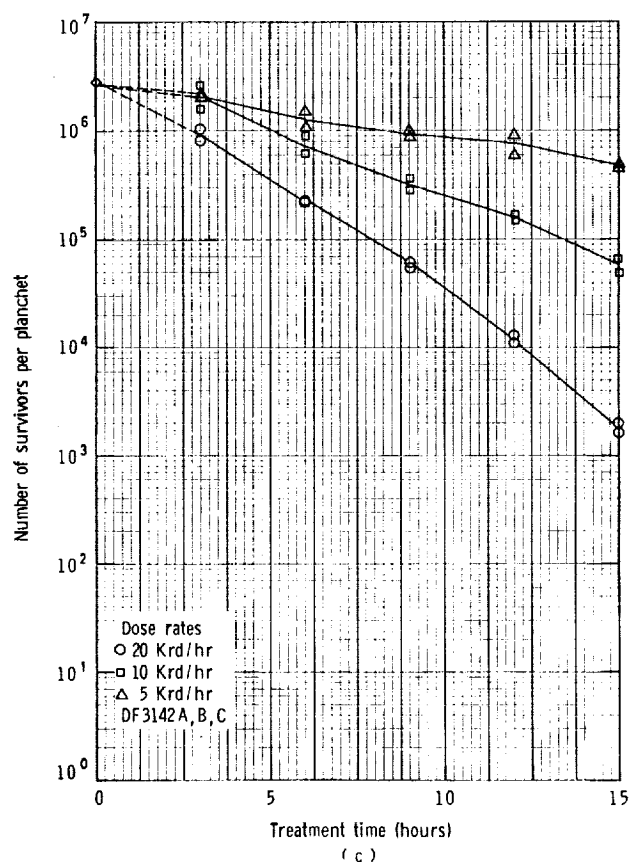
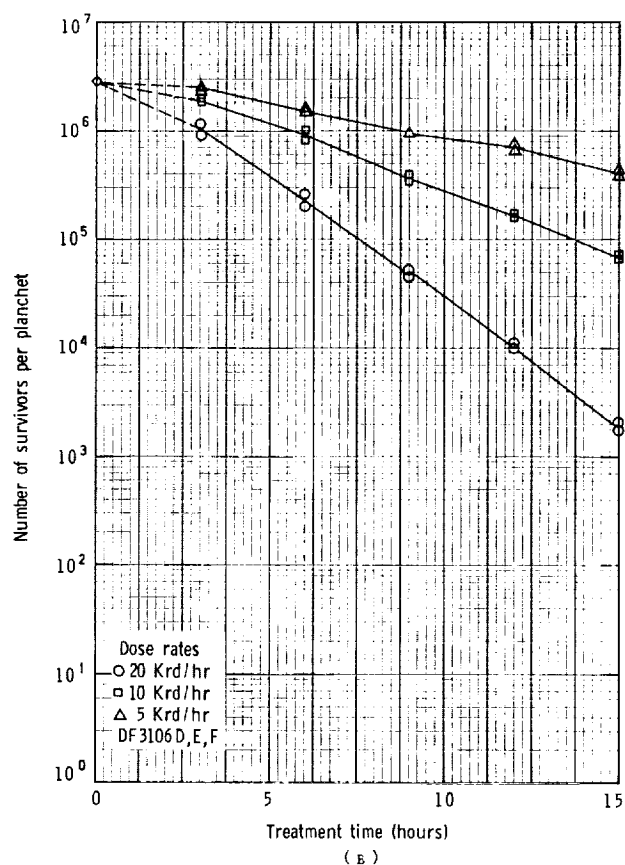
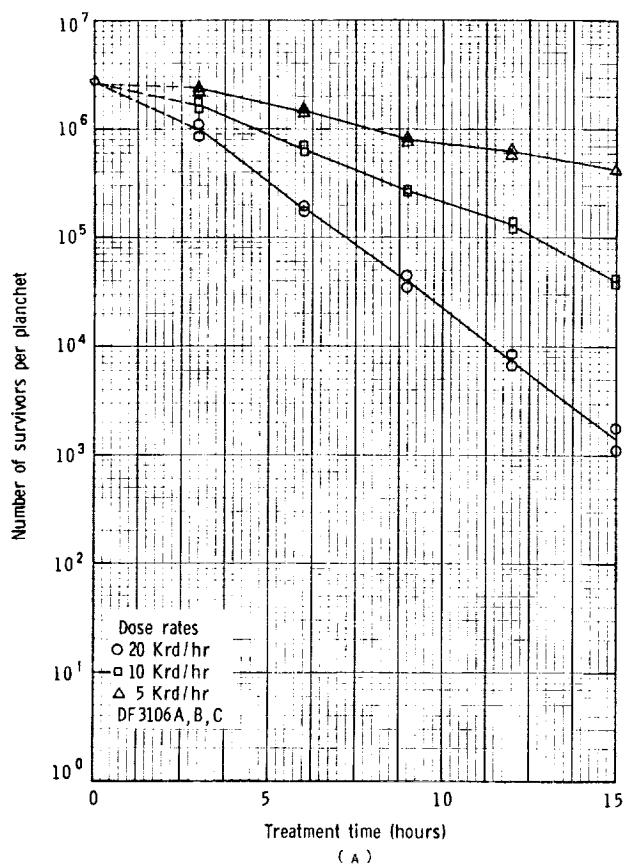


FIGURE 1.5: SURVIVOR CURVES FOR (DRY) RADIATION OF BACILLUS SUBTILIS VAR. NIGER (AANK) AT 27°C AND 50% RH

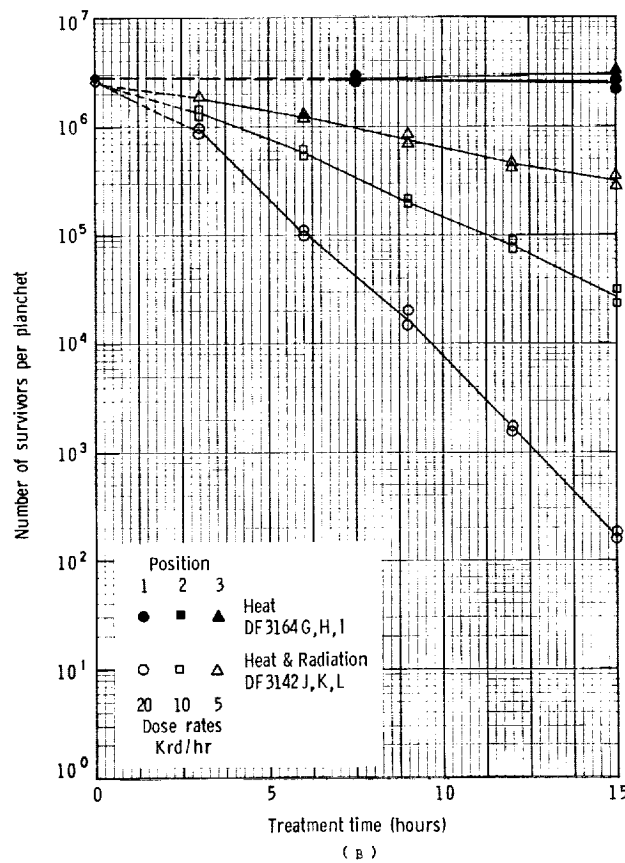
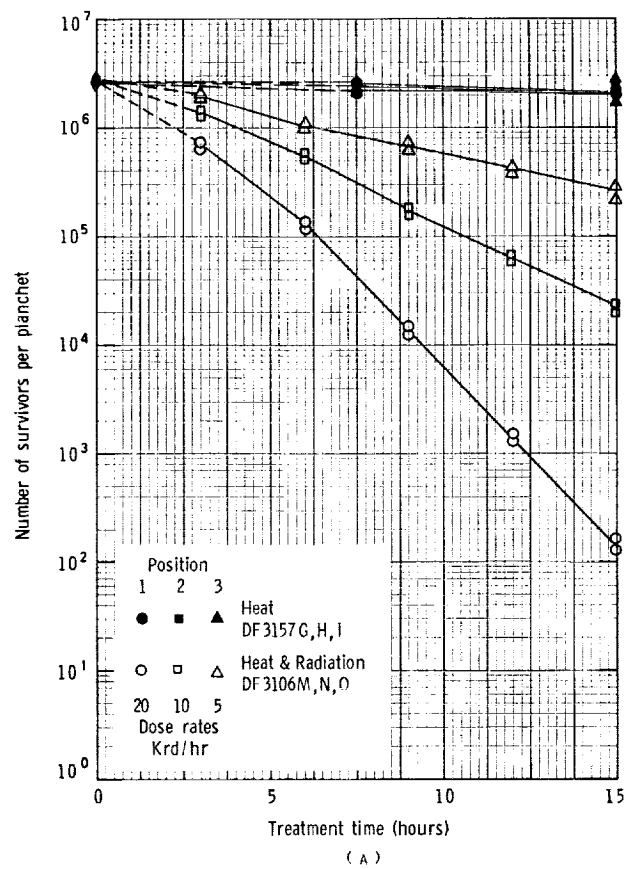


FIGURE 1.6: SURVIVOR CURVES FOR DRY-HEAT THERMAL AND THERMORADIATION TREATMENT OF *BACILLUS SUBTILIS* VAR. JIGER (AAHK) AT 75°C AND 52% RH

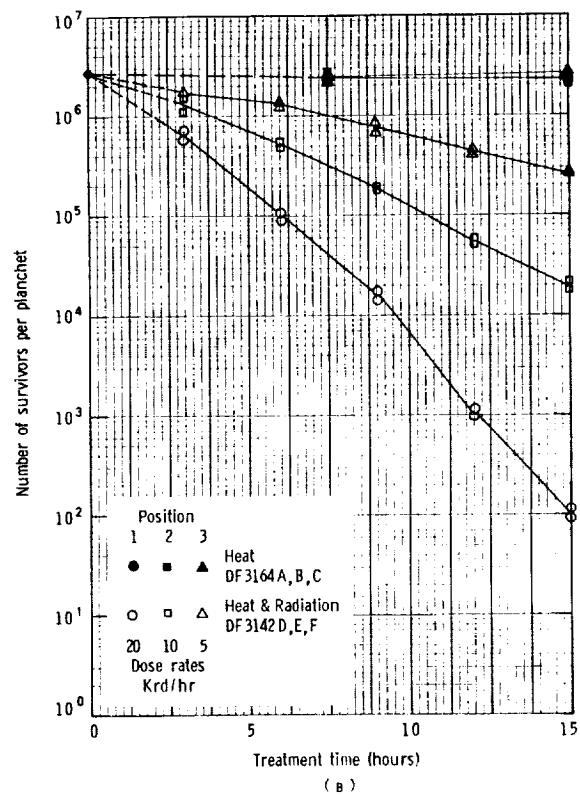
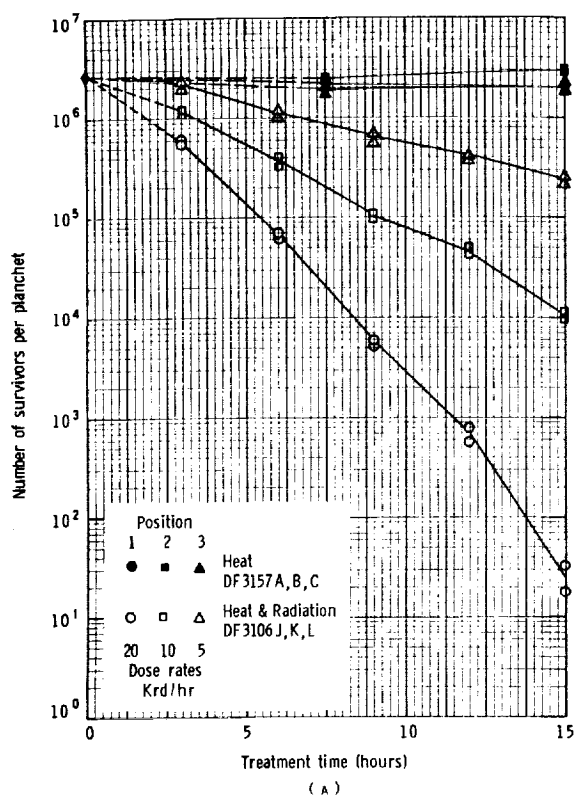


FIGURE 1.7: SURVIVOR CURVES FOR DRY-HEAT THERMAL AND THERMORADIATION TREATMENT OF *BACILLUS SUBTILIS* VAR. *NIGER* (AAHK) AT 90°C AND 28% RH

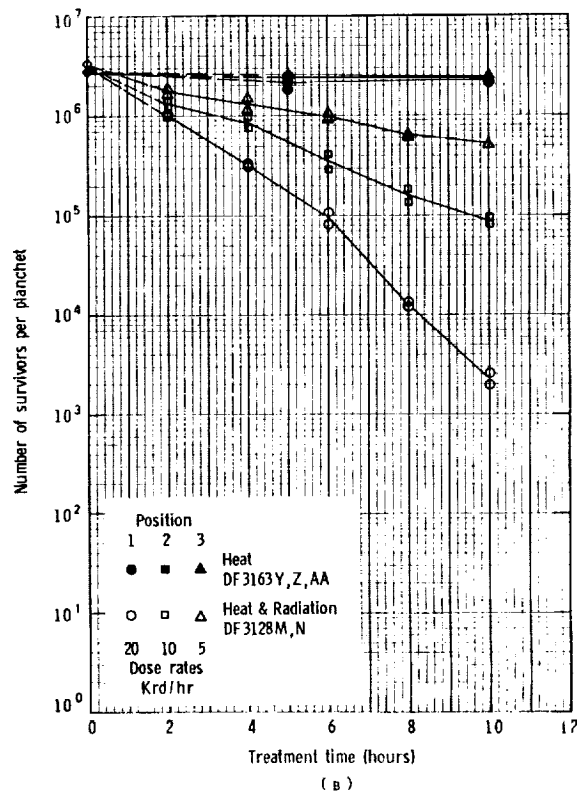
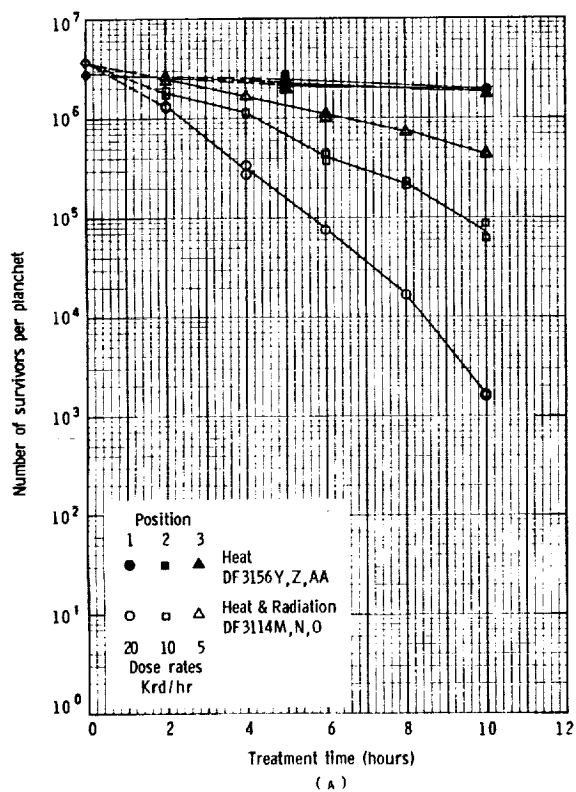


FIGURE 1.8: SURVIVOR CURVES FOR DRY-HEAT THERMAL AND THERMORADIATION TREATMENT OF *BACILLUS SUBTILIS* VAR. *NIGER* (AAHK) AT 90°C AND 55% RH

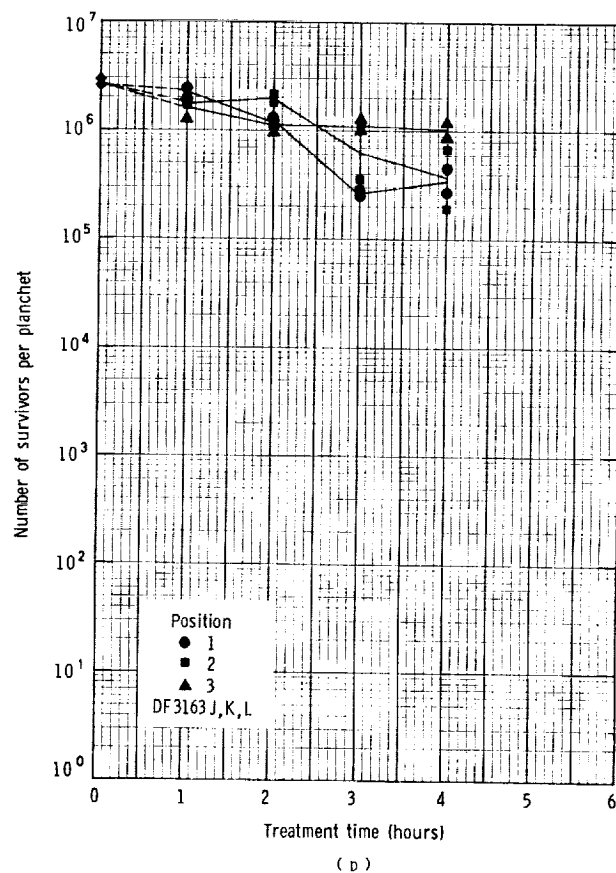
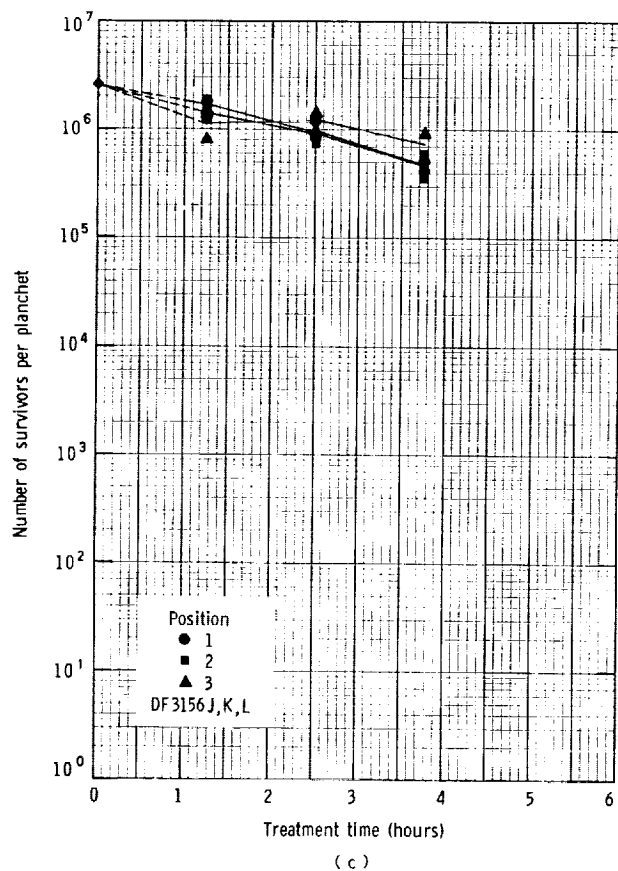
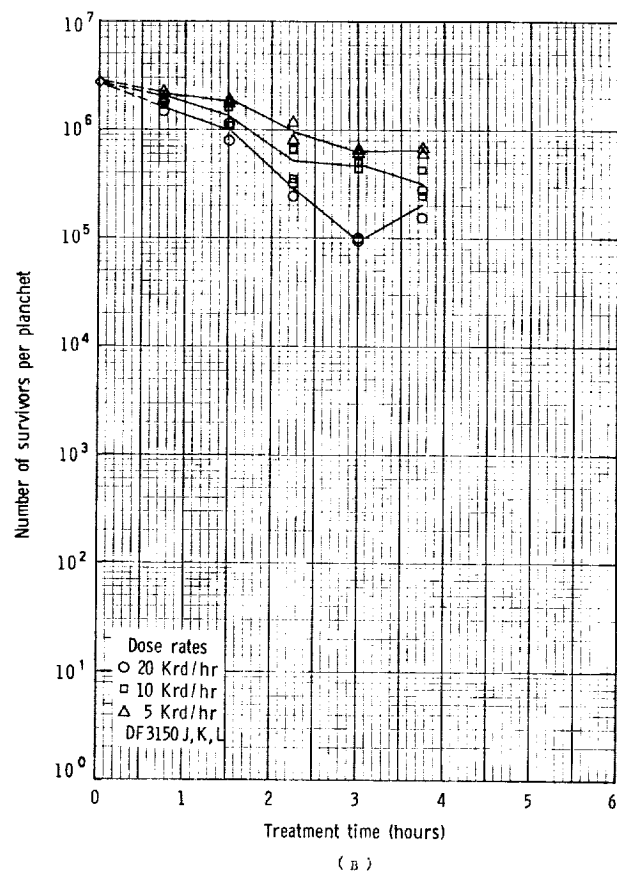
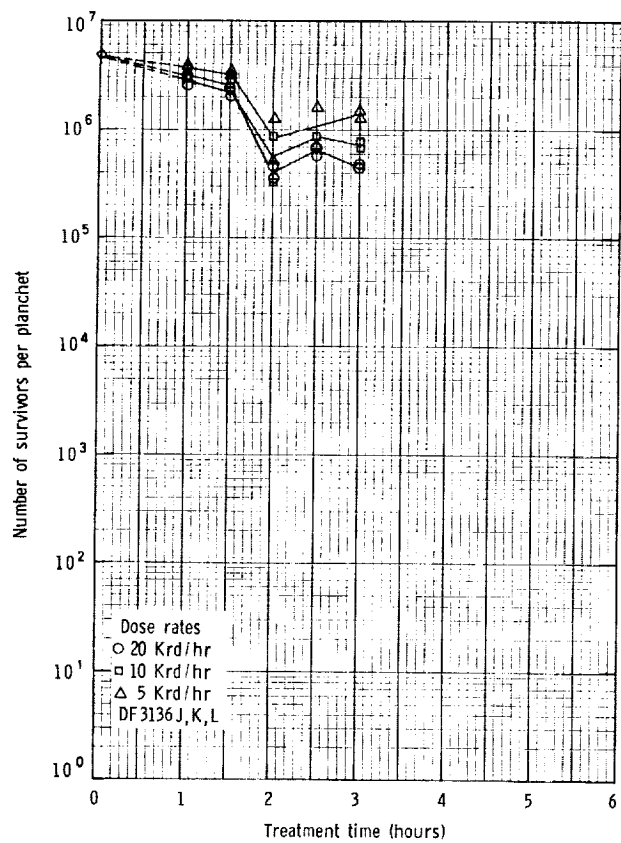


FIGURE 1.9: SURVIVOR CURVES FOR DRY-HEAT THERMORADIATION
 [(A) AND (B)] AND THERMAL [(C) AND (D)]
 TREATMENT OF *BACILLUS SUBTILIS* VAR. *NIGER*
 (AAHK) AT 90°C AND 82% RH

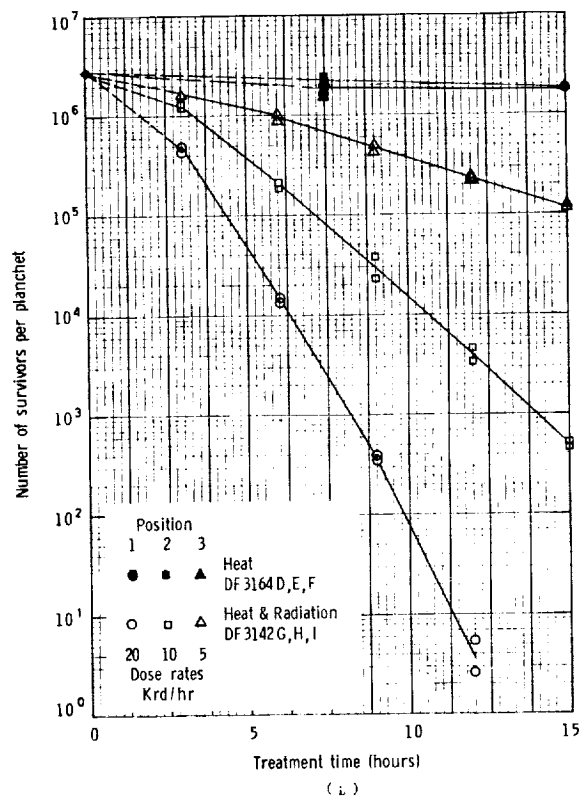
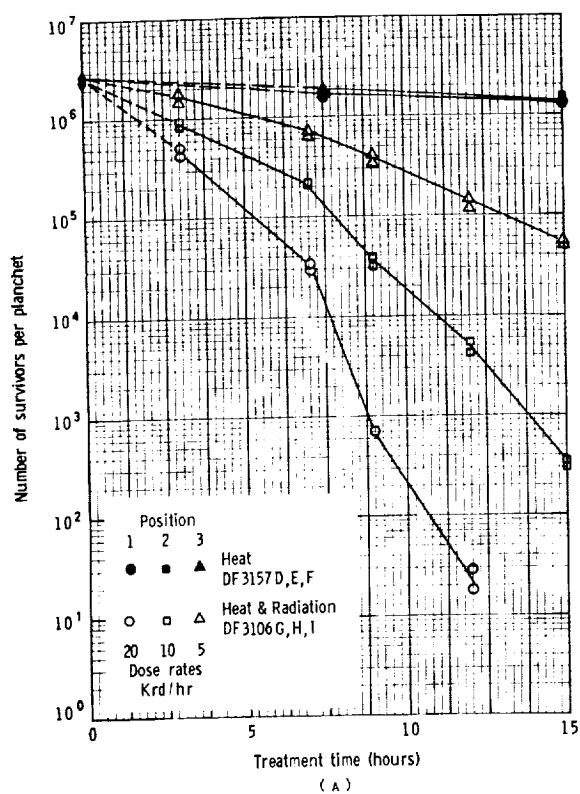


FIGURE 1.10: SURVIVOR CURVES FOR DRY-HEAT THERMAL AND THERMORADIATION TREATMENT OF BACILLUS SUBTILIS VAR. NIGER (AAHK) AT 105°C AND 17% RH

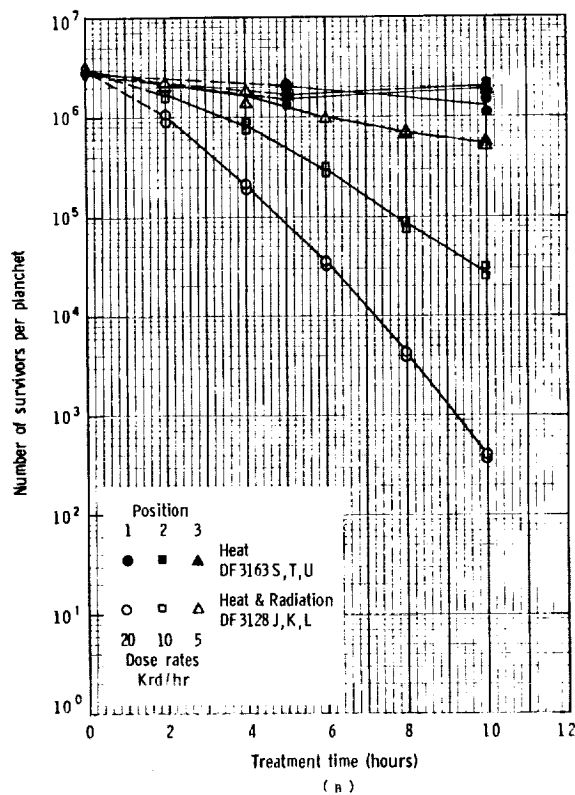
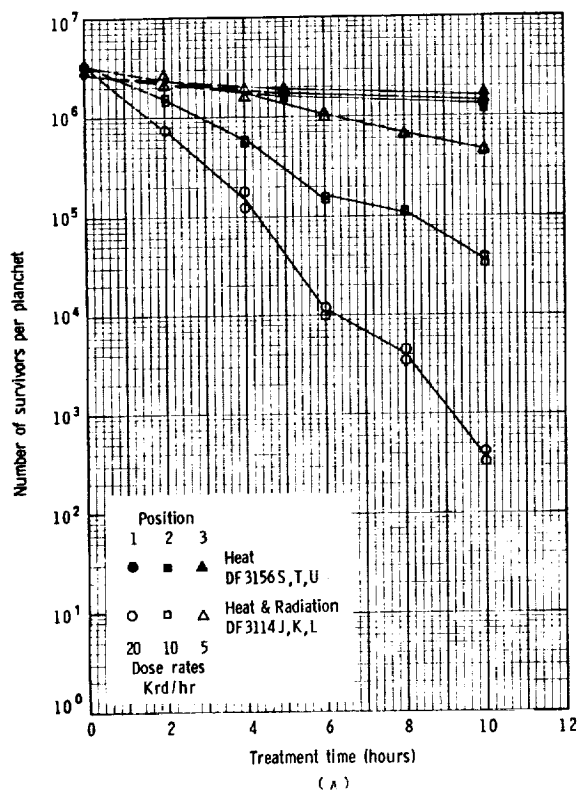


FIGURE 1.11: SURVIVOR CURVES FOR DRY-HEAT THERMAL AND THERMORADIATION TREATMENT OF BACILLUS SUBTILIS VAR. NIGER (AAHK) AT 105°C AND 32% RH

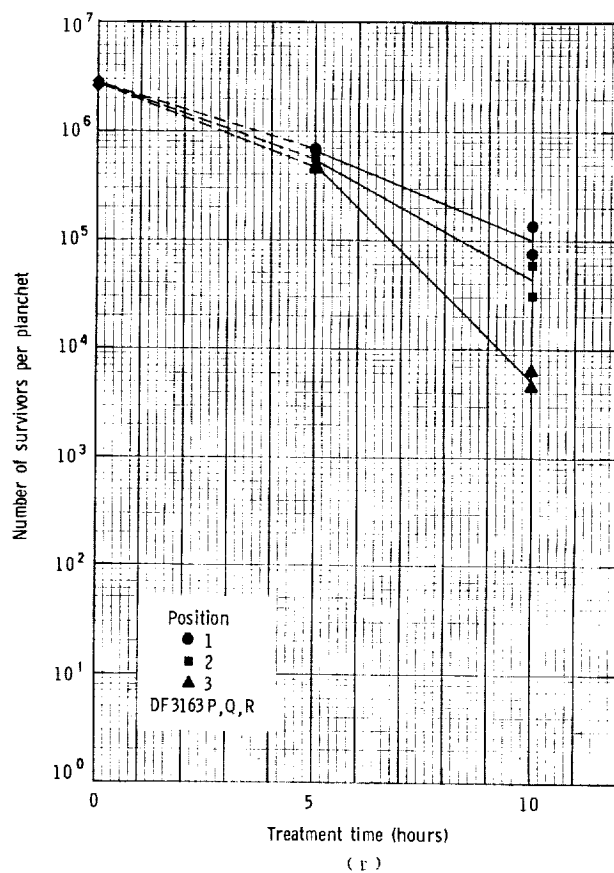
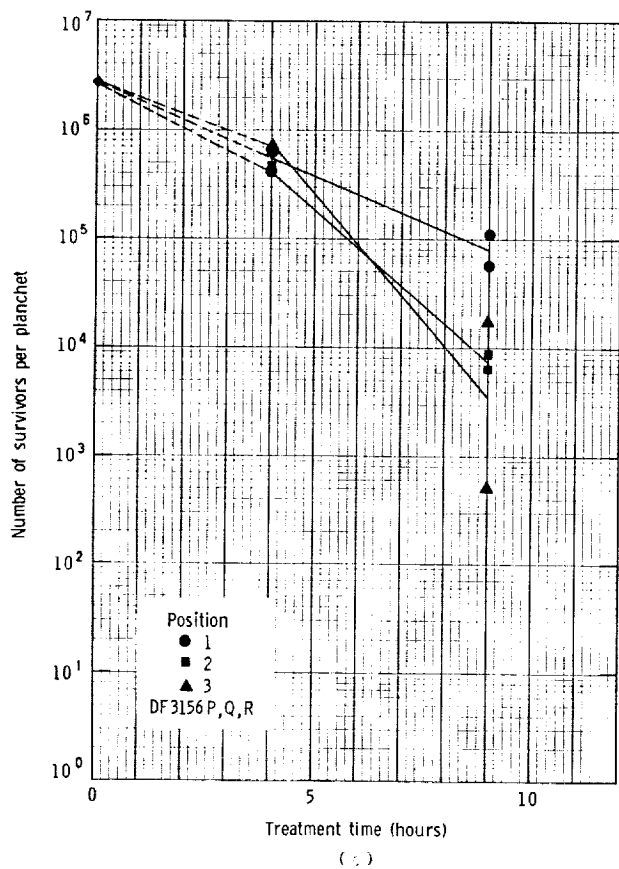
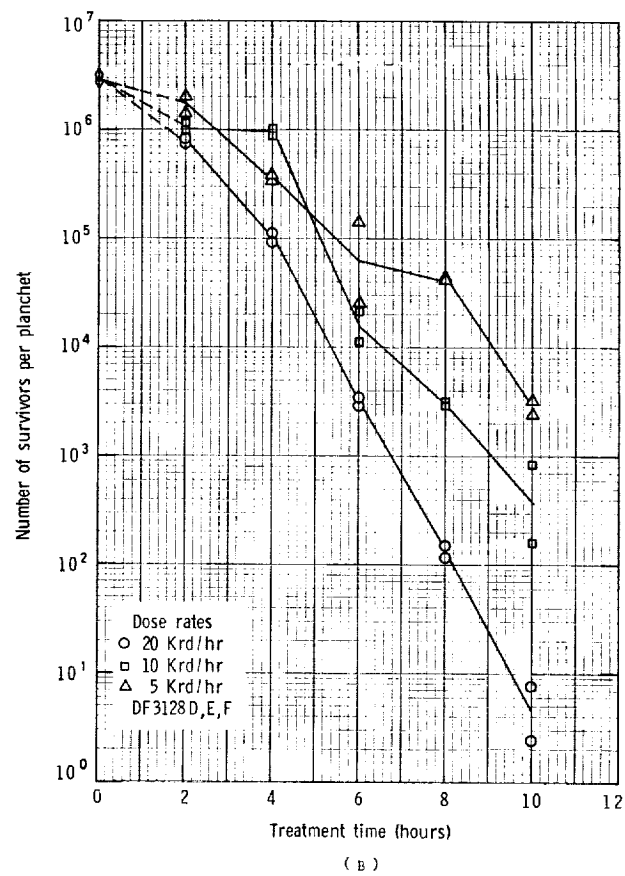
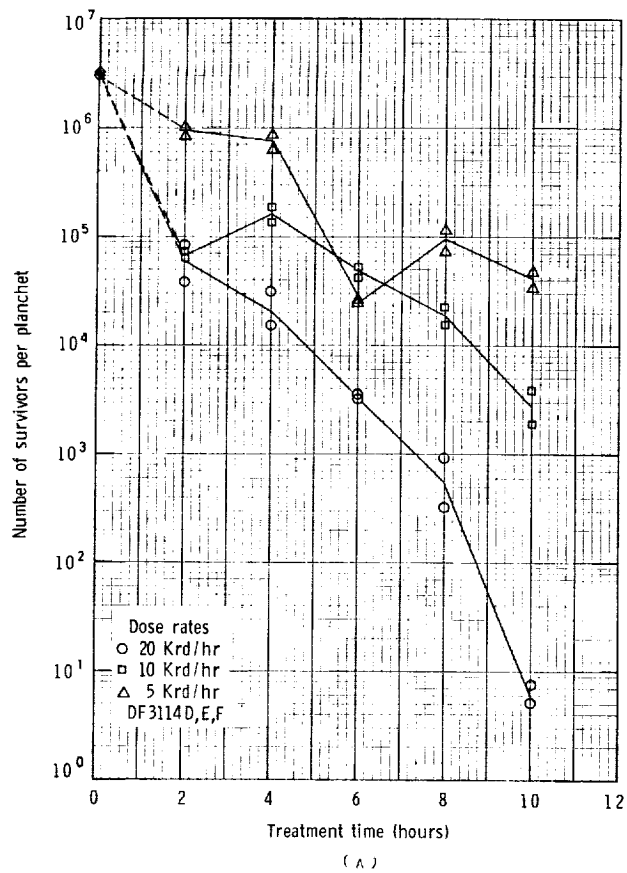


FIGURE 1.12: SURVIVOR CURVES FOR DRY-HEAT THERMORADIATION [(A) AND (B)] AND THERMAL [(C) AND (D)] TREATMENT OF *BACILLUS SUBTILIS* VAR. *NIGER* (AAHK) AT 105°C AND 58% RH

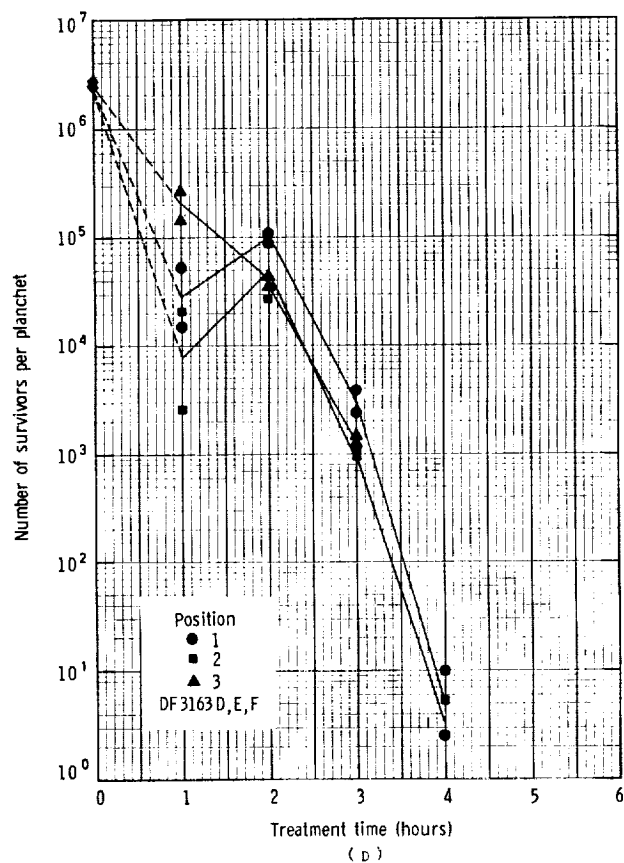
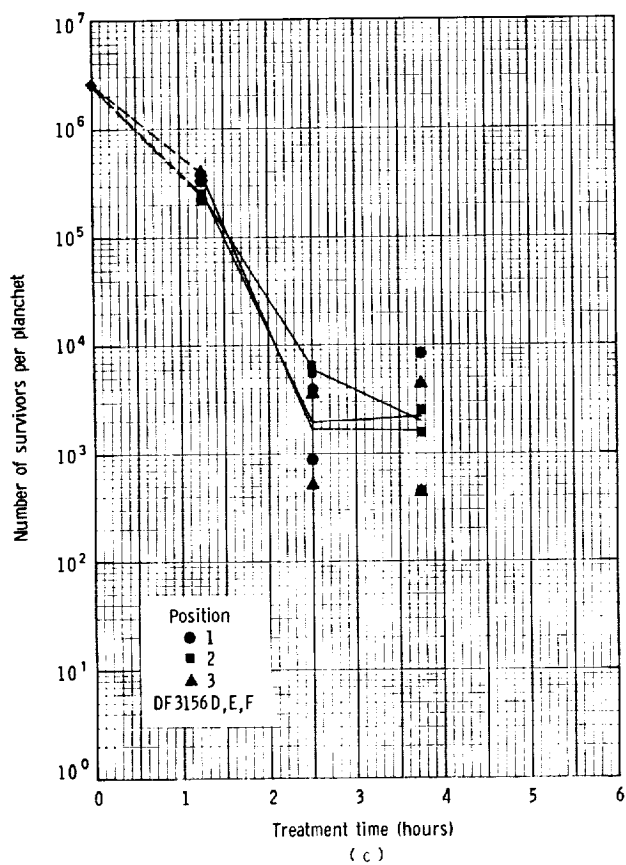
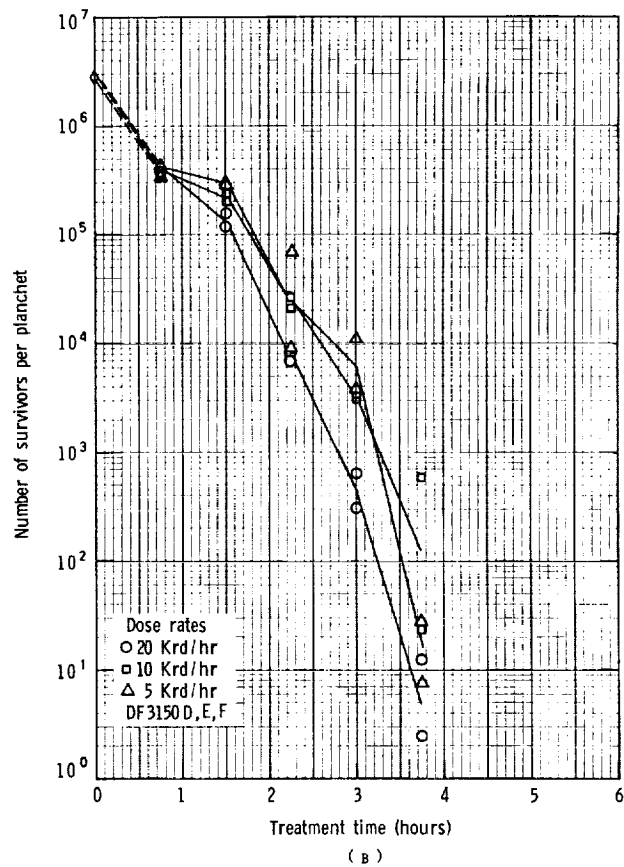
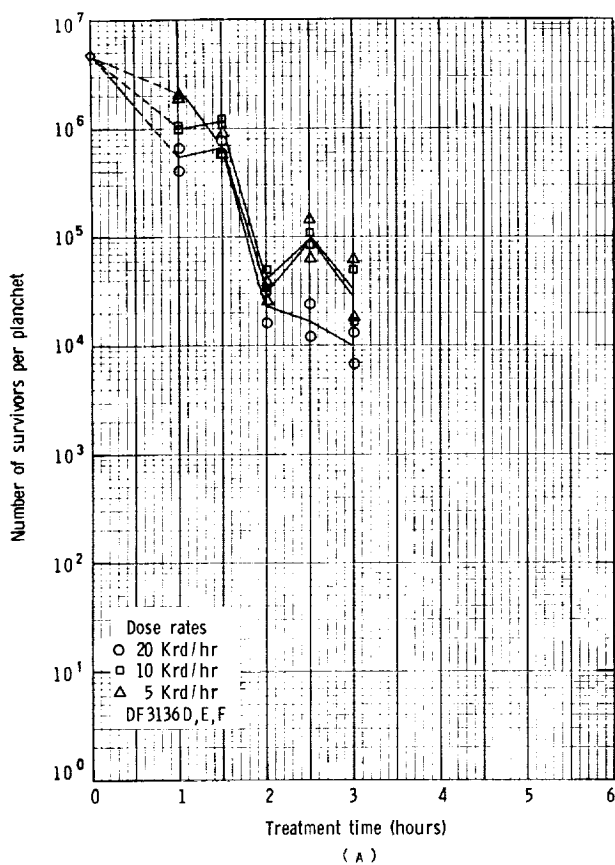


FIGURE 1.13: SURVIVOR CURVES FOR DRY-HEAT THERMORADIATION [(A) AND (B)] AND THERMAL [(C) AND (D)] TREATMENT OF *BACILLUS SUBTILIS* VAR. *NIGER* (AAHK) AT 105°C AND 70% RH

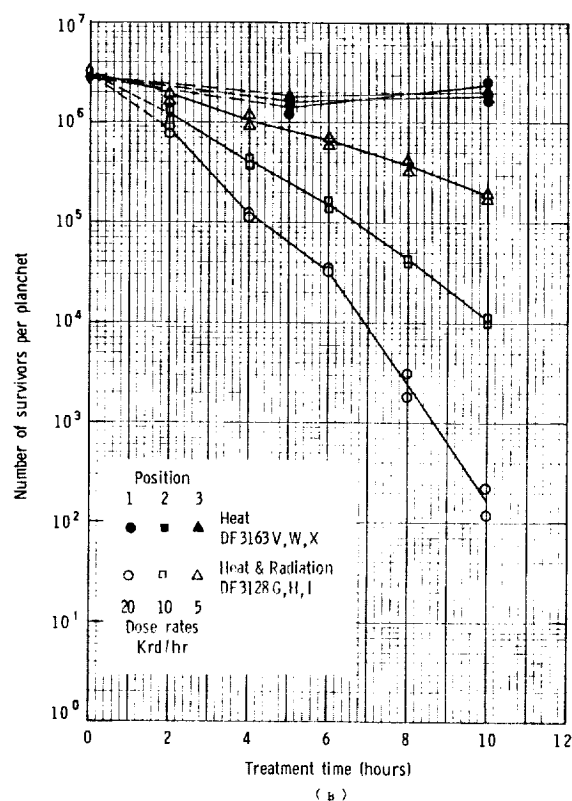
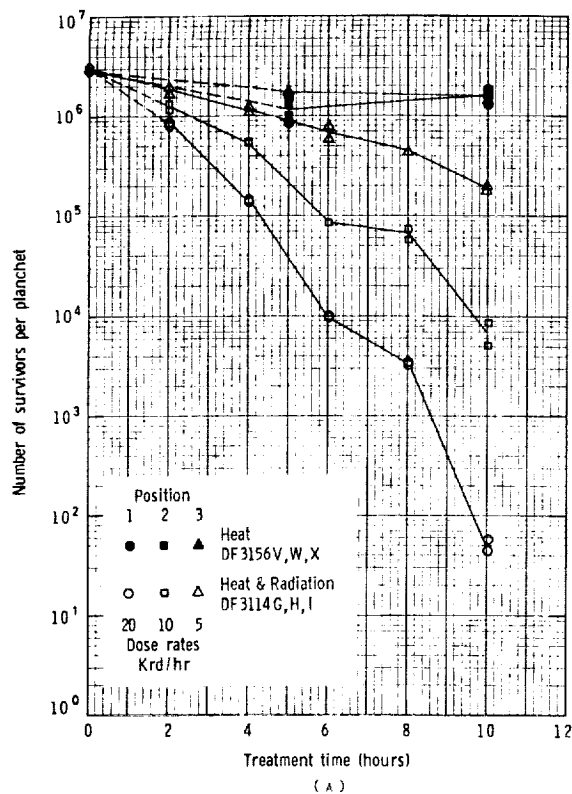


FIGURE 1.14: SURVIVOR CURVES FOR DRY-HEAT THERMAL AND THERMORADIATION TREATMENT OF *BACILLUS SUBTILIS* VAR. *NIGER* (AAHK) AT 110°C AND 27% RH

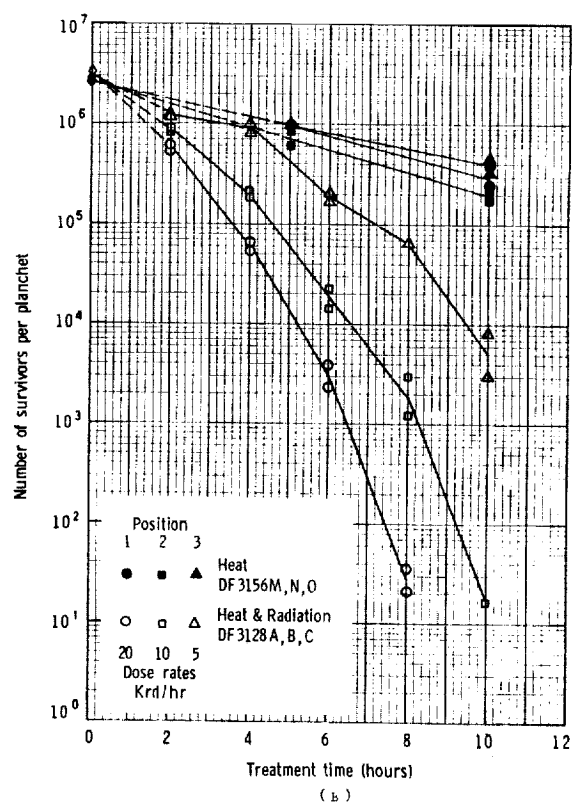
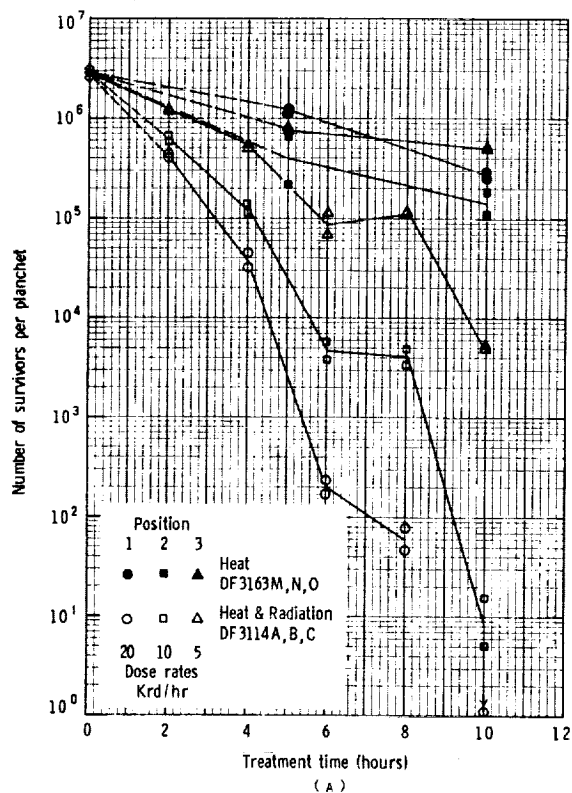


FIGURE 1.15: SURVIVOR CURVES FOR DRY-HEAT THERMAL AND THERMORADIATION TREATMENT OF *BACILLUS SUBTILIS* VAR. *NIGER* (AAHK) AT 110°C AND 49% RH

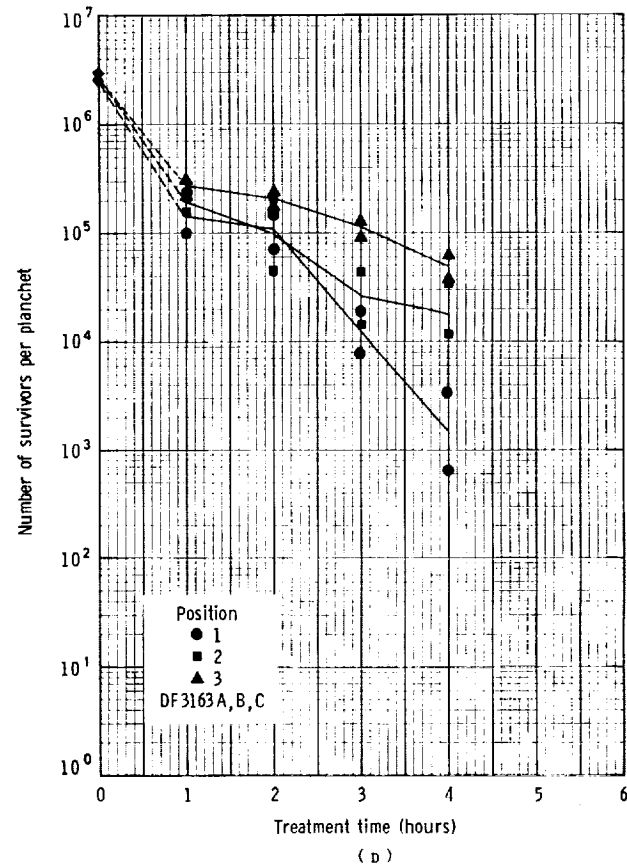
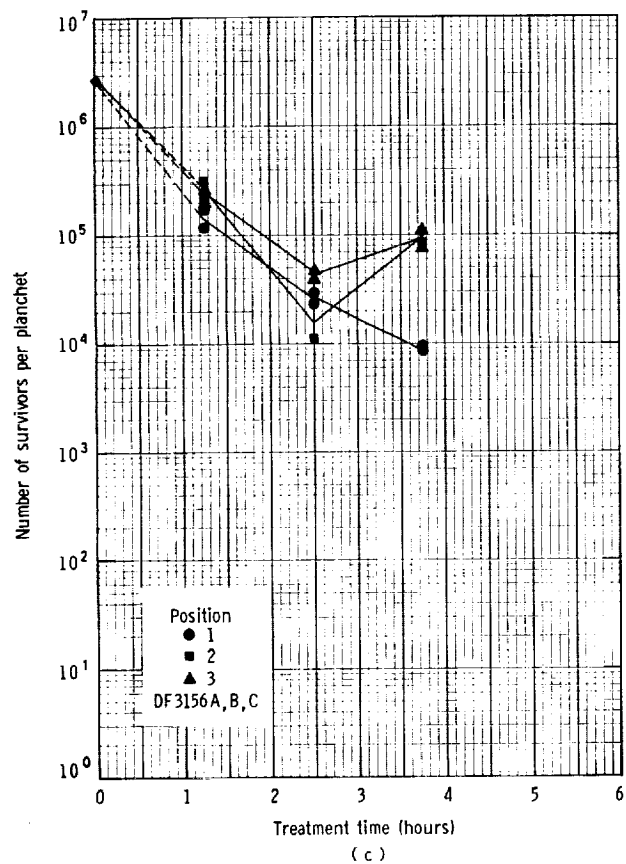
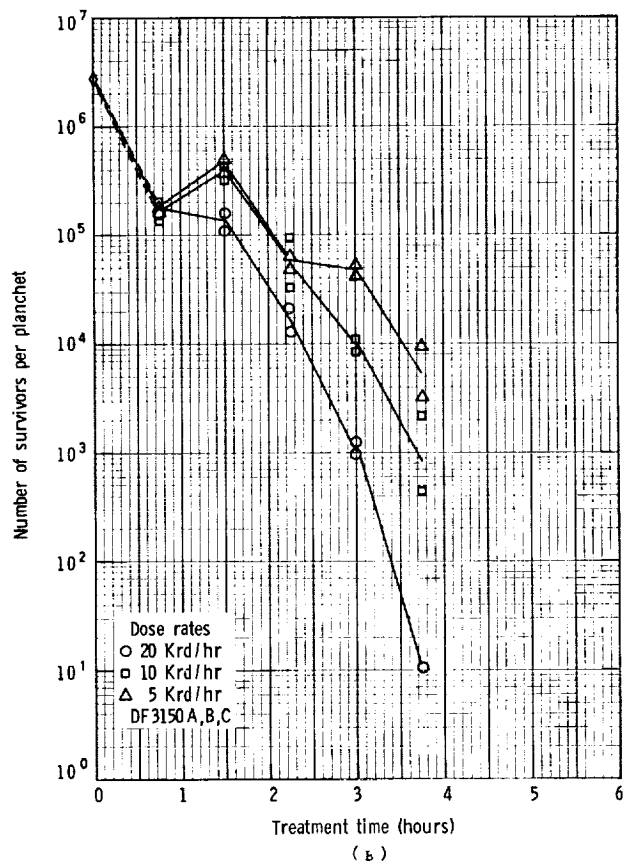
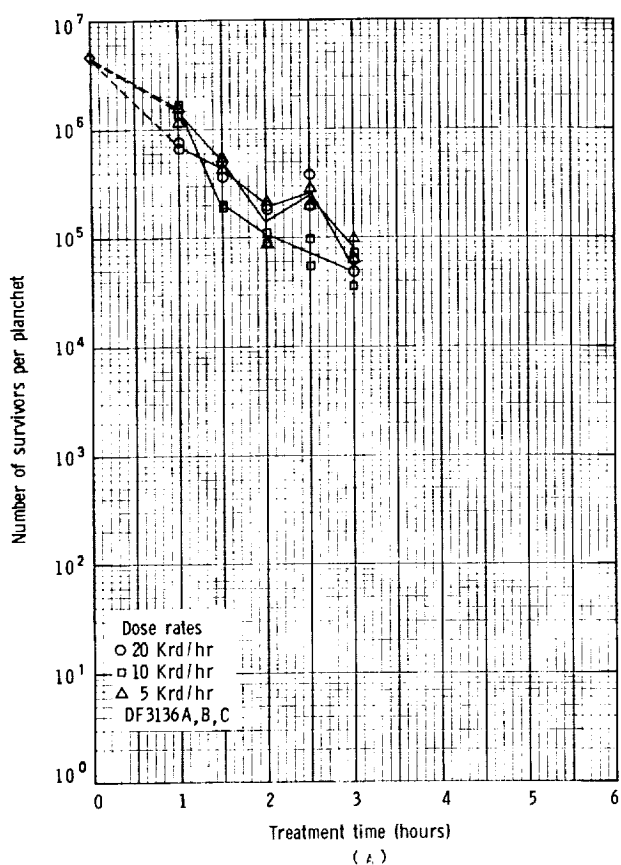


FIGURE 1.16: SURVIVOR CURVES FOR DRY-HEAT THERMORADIATION [(A) AND (B)] AND THERMAL [(C) AND (D)] TREATMENT OF *BACILLUS SUBTILIS* VAR. NIGER (AAHK) AT 110°C AND 59% RH

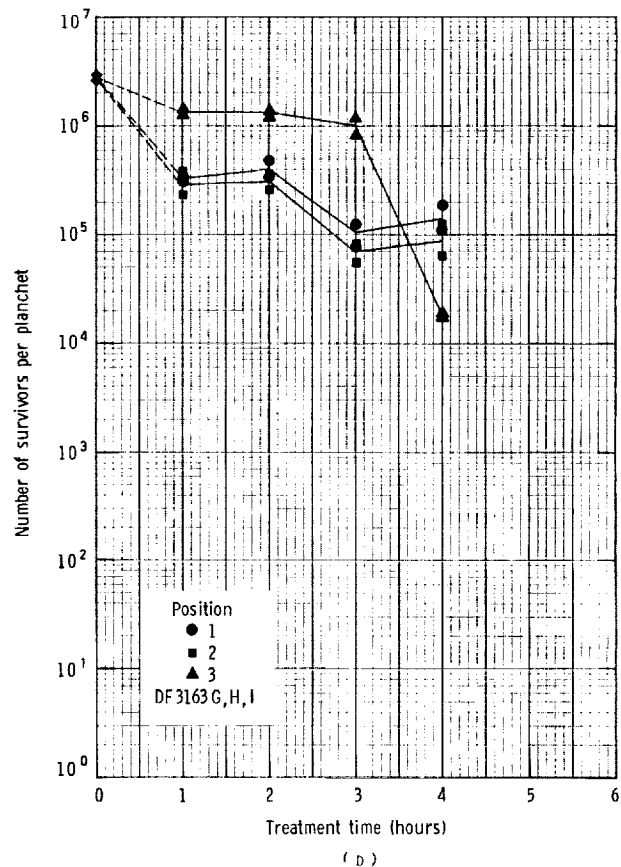
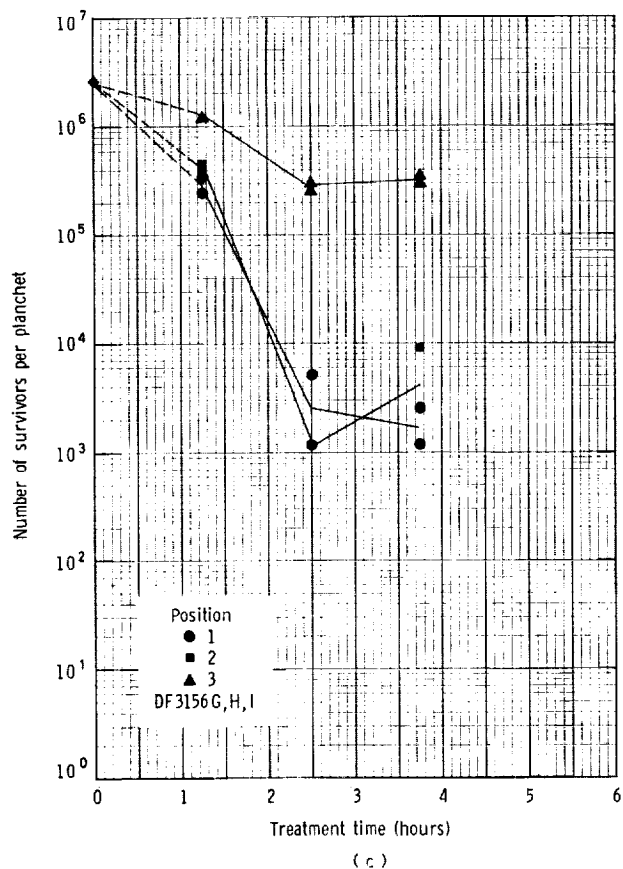
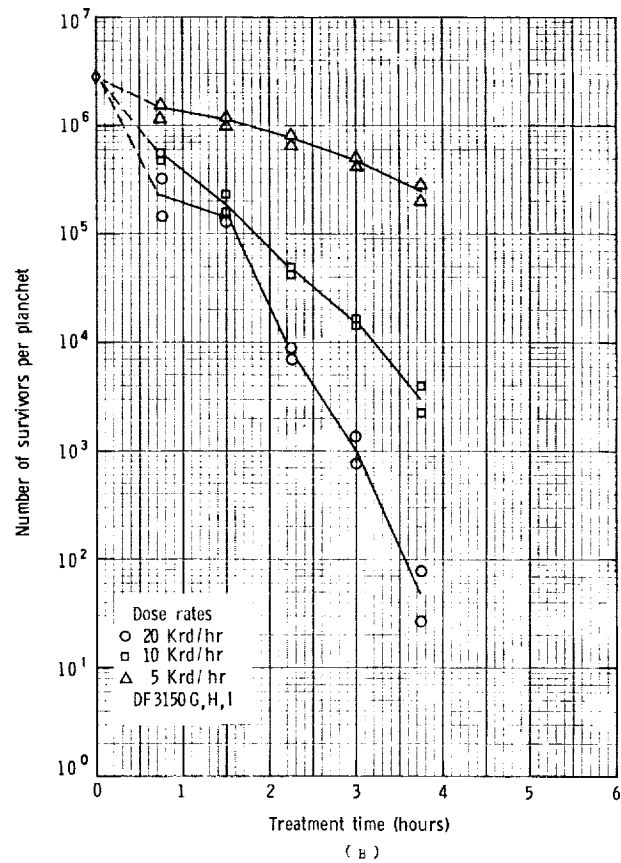
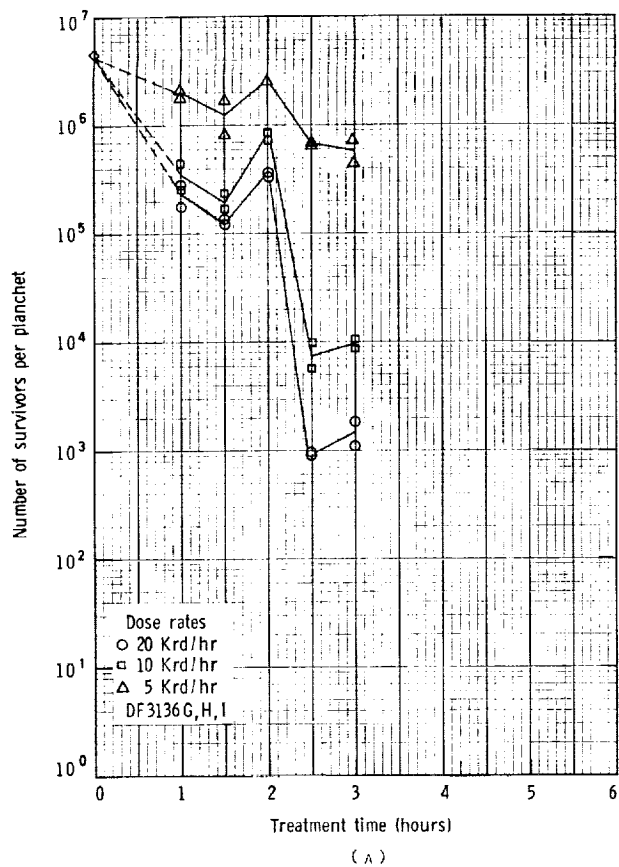


FIGURE 1.17: SURVIVOR CURVES FOR DRY-HEAT THERMORADIATION [(A) AND (B)] AND THERMAL [(C) AND (D)] TREATMENT OF *BACILLUS SUBTILIS* VAR. *HIGER* (AAHK) AT 125°C AND 25% RH

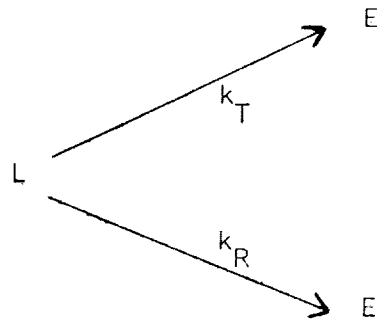
also plotted for experiments where heat was the only lethal agent at the same psychrometric condition. One should keep in mind that these results are from a different experiment performed on a different day than the thermoradiation experiment. For the thermoradiation experiment, results are shown for survival levels measured at each of the three positions used in thermoradiation testing. The symbol shape remains consistent between thermal results and thermoradiation results for a given position. The results of replicate experiments appear in adjacent graphs.

DISCUSSION

The discussion of the results of the thermoradiation experimentation will cover the following topics: (1) Terms will be defined for certain details and parameters of the experimental work; (2) Reduction of the experimental data to examine the effects that each of the independent stresses have on the final death rate; (3) A discussion of the general mechanistic characteristics of both heat and radiation; (4) Proposal of two models for the thermoradiation process which incorporate the salient features of the overall process. The mathematical simulation of one model is described and its characteristics are explored and compared with the experimental data.

Definition of Terms

At the most general level a thermoradiation sterilization process can be schematically represented as:



L represents viable spores.

E represents a dead spore.

k_T is the kinetic parameter attributed to thermal destruction processes.

k_R is the kinetic parameter attributed to all remaining death mechanisms which are not effective unless radiation is present.

Therefore the following definitions seem appropriate and convenient.

Thermal experiment - an experiment where heat is the only lethal agent.

Radiation experiment - an experiment where lethal conditions are provided only by gamma radiation.

Thermoradiation experiment - an experiment which has both heat and radiation operating to kill spores.

D_{TR} - The D-value calculated from the least square regression to a set of data from a thermoradiation experiment.

D_T - the D-value measured from a thermal experiment. For an apparent first order reaction, $D_T = 2.303/k_T$.

D_R - The D-value calculated from thermoradiation experiments for decrease in spore population resulting from mechanisms present in thermoradiation experiments which are not present in the comparable thermal experiment. Therefore values of D_R at a particular condition are calculated from corresponding values of D_{TR} and D_T according to:

$$\frac{1}{D_R} = \frac{1}{D_{TR}} - \frac{1}{D_T} \quad (1.1)$$

D_{R0} - The D-value for the radiation experiment, i.e., radiation at ambient temperatures.

Therefore, synergism becomes apparent when D_R (or the D-value for the portion of death which is present in a thermoradiation experiment but not present in a thermal experiment) is less than D_{R0} .

D_{R0} naturally has a temperature dependency of the Arrhenius form over a range of temperatures far below heat sterilization temperature range. The energy of activation for this dependency was measured by Webb, Ehret, and Powers (1958) to be 110 cal/mole over the range -143 to 36°C in Bacillus megaterium. Therefore, if the mechanisms were merely additive we would expect to find an energy of activation in this range.

Data Reduction

The semi-logarithmic survivor curves shown in Figures 1.5 through 1.17 are generally linear in shape. There appears to be a trend for the semilogarithmic survivor curves to be less linear at high relative humidity levels. Although some of the semi-logarithmic survivor graphs

are curves and not straight lines we feel that the only practical approach to analysis is to fit a straight line to the semi-logarithmic survivor curve data by least square linear regression. Having established this line we can determine the values of D_{TR} for any combination of heat and radiation.

Figures 1.18, 1.19, and 1.20 show the resulting values of D_{TR} for temperatures of 90°, 105° and 110°C over the range of relative humidity and Figure 1.21 shows a similar plot of D_T over the range of conditions examined. The isothermal curves for D_T over the range of relative humidities follow the general pattern that is expected in dry heat sterilization; namely that the D-value decreases rapidly with increasing relative humidity. Curves for successively higher temperatures fall below one another but are similar in shape. The graphs of D_{TR} over the range of relative humidities for 105° and 110°C show a similar shape. At low relative humidities, the vertical distance between curves for a two-fold increase in dose rate is approximately equal to $\log(2)$. At the higher relative humidities the curves converge sharply as the heat sterilization mechanism becomes more significant.

We can uncouple the radiation effect from the thermoradiation data by using Equation 1.1. The value of D_T used in this calculation is the geometric mean of D_T 's calculated from replicated experiments measured at the same location in the environmental chamber where a given dose rate is experienced and at the the same psychrometric condition. The values of D_R calculated in this fashion are shown in Figures 1.22 through 1.23 for each temperature examined.

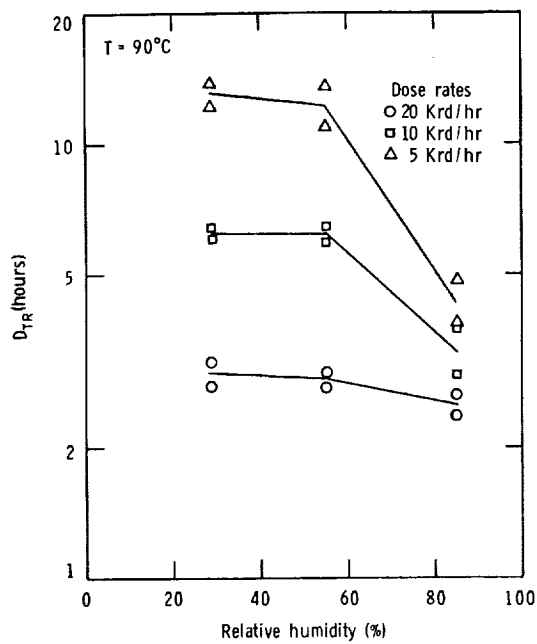


FIGURE 1.18: D_{TR}-VALUES FOR THERMORADIATION TREATMENT OF *BACILLUS SUBTILIS* VAR. *NIGER* (AWK) AT DIFFERENT RELATIVE HUMIDITIES AND 90°C.

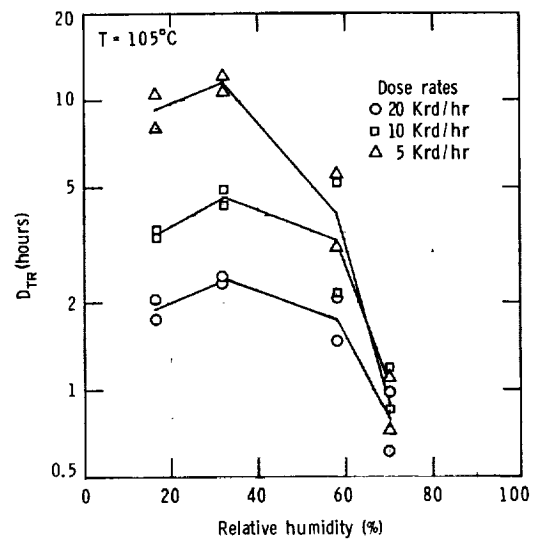


FIGURE 1.19: D_{TR}-VALUES FOR THERMORADIATION TREATMENT OF *BACILLUS SUBTILIS* VAR. *NIGER* (AWK) AT DIFFERENT RELATIVE HUMIDITIES AND 105°C.

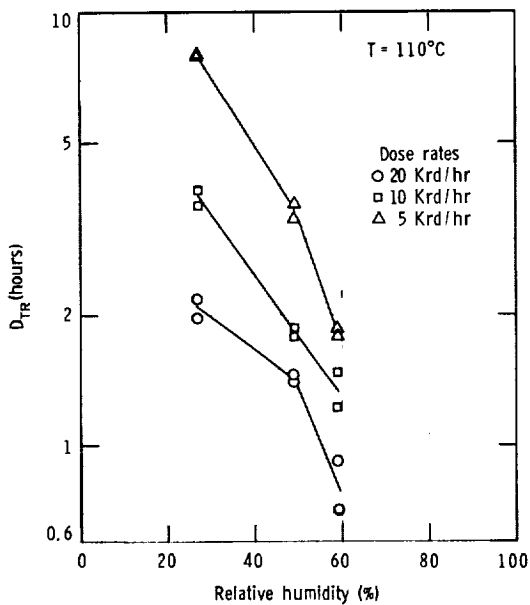


FIGURE 1.20: D_{TR}-VALUES FOR THERMORADIATION TREATMENT OF *BACILLUS SUBTILIS* VAR. *NIGER* (AWK) AT DIFFERENT RELATIVE HUMIDITIES AND 110°C.

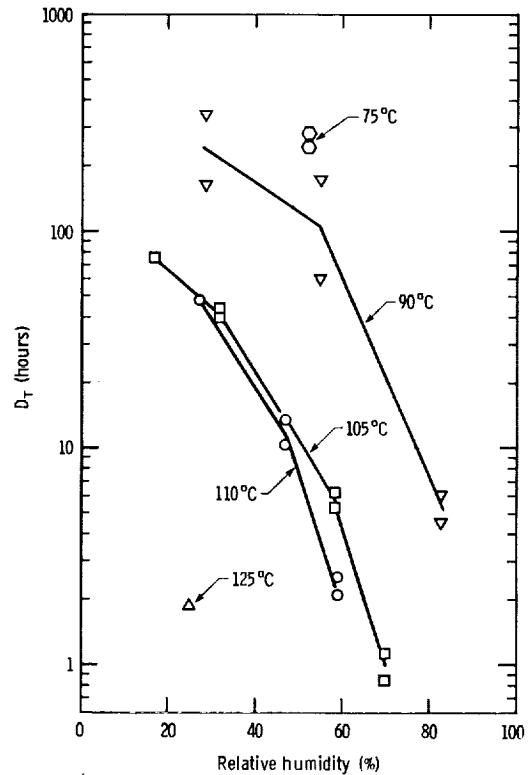


FIGURE 1.21: D_T-VALUES FOR THERMAL TREATMENT OF *BACILLUS SUBTILIS* VAR. *NIGER* (AWK) AT VARIOUS TREATMENT TEMPERATURES OVER RANGE OF RELATIVE HUMIDITIES.

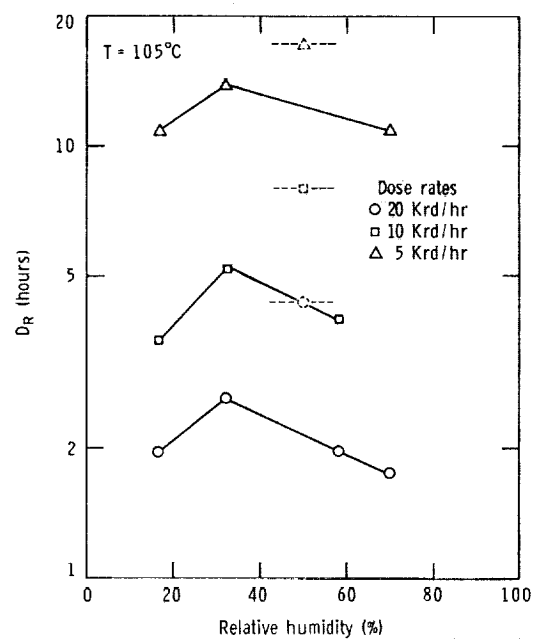


FIGURE 1.22: D_R -VALUES CALCULATED FROM THERMORADIATION TREATMENT OF *BACILLUS SUBTILIS* VAR. NIGER (AHHO) AT VARIOUS RELATIVE HUMIDITIES AND 105°C . (DASHED RESULTS ARE RESULTS FROM RADIATION TREATMENT AT 27°C AND 50% RH.)

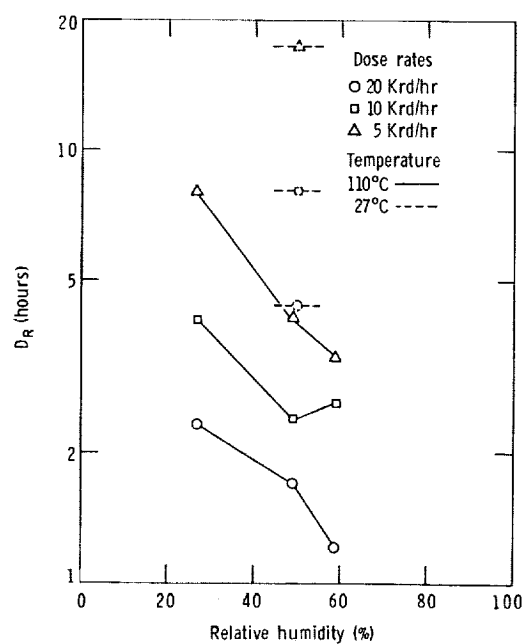


FIGURE 1.23: D_R - VALUES CALCULATED FROM THERMORADIATION TREATMENT OF *BACILLUS SUBTILIS* VAR. NIGER (AHHO) AT VARIOUS RELATIVE HUMIDITIES AND 110°C . (DASHED RESULTS ARE RESULTS FROM RADIATION TREATMENT AT 27°C AND 50% RH.)

For any temperature, D_R shows a relative humidity dependency although somewhat weaker than D_T . The vertical distance between curves for a two-fold dose rate change is approximately equal to $\log(2)$ over the entire range.

We can compare values of D_R calculated from thermoradiation experiments with the value D_{R0} measured from the radiation experiments. Values of D_{R0} are indicated by dashed lines in Figures 1.22 through 1.23. The values of D_R are consistently lower than D_{R0} . The differences between D_R and D_{R0} represent the resultant kill by mechanisms which are not present with radiation at ambient temperature and therefore contribute to the synergistic effect of thermoradiation.

Thus, we see from these data that the amount of synergism is dependent on the relative humidity level as well as temperature.

Apparently, the resulting synergism effect on the rate of microbial spore inactivation, when heat and radiation are jointly applied, has properties of each of the individual agents; namely a dependency on dose rate similar to the radiation dependency and a dependency on relative humidity similar to a dry-heat process.

Mechanistic Analysis

An intriguing question which is still open to speculation and interpretation is: What is the basis for the synergistic effect? We will briefly outline two proposed models which display several of the properties of synergistic effect.

Background - Much work by previous investigators has been devoted to attempts at explaining the mechanism of death, for both thermal processes and radiation processes, in light of the biochemical events which lead to the inability of a spore to reproduce given favorable conditions. It is generally believed for both heat and radiation processes that the cellular function is interrupted by denaturation or degradation of a critical protein. The exact nature of the attack by the lethal agent remains unsettled.

Thermal Mechanisms - Heat sterilization generally has been interpreted as being a result of denaturation of a critical molecule. In this case denaturation would mean breaking down of a physical form of the critical molecule, primarily by severing hydrogen bonds that exist between different portions of the critical macromolecular structure.

The role of water activity enters very strongly in this type of mechanism. Focusing our attention on a spore in an extremely dry state, as water vapor surrounding the spore increases, the amount of bound water in the spore increases. The limited amount of water selectively binds at sites on the macromolecule and acts as a bridge between different portions of the molecule where the cement on either end of the bridge is a physical bond (hydrogen bond). Thus, as more water is added, the amount of hydrogen bonding increases adding to the physical integrity of the macromolecule.

After a certain point, however, additional water in the spores no longer acts as a bonding agent. At this point the bonding sites are saturated and additional water starts to fill regions outside these areas. The presence of additional water in these areas apparently

detracts from the effectiveness of the water that is already bound; thus, the dipole field of the unbound water is enough to disrupt the relatively weak hydrogen bonds of some bound water, thereby lessening the physical integrity of the macromolecule and making it more vulnerable to either denaturation or degradation by thermal activities.

Therefore, we see the physical state of the molecule passing through a state of maximum integrity where it can withstand higher thermal excitations before breaking down by either a denaturation or a degradation process.

Radiological Mechanisms - in the presence of ionizing radiation, the critical molecule may be rendered inoperative by one or two distinct mechanisms; the macromolecule itself is ionized either by the passage of an electron or by indirect action where the radiation primarily influences another molecule which in turn attacks the critical molecule.

The role of water in radiation mechanisms is much less apparent than in a heat mechanism. Free water is capable of being ionized and thereafter breaking down into free radicals by radiation. However, the free path of such a radical is relatively short; therefore, the probability of reaction between the radicals and the critical molecule is minimal.

Radiation ionization of bound water affects the macromolecule to which the water is bound. The free radicals created from the water subsequently can react with the molecule. However, this mechanistic route is of little consequence compared with the direct action of the radiation on the macromolecule since the target size (molecular weights and amounts) of bound water is comparatively small.

Mechanisms Compared - in consideration of radiological effects, both direct and indirect mechanisms appear to produce irreversible changes in the chemical structure of the macromolecule. On the other hand, thermal mechanisms produce changes which are chemically reversible until a critical number of steps have been achieved after which subsequent changes are irreversible.

Model Number 1

It seems plausible that, with both types of mechanisms, more than one bond must be broken before the macromolecule and consequently the microorganisms is inactivated. Cox and Peacocke (1957) show that for denaturation of DNA isolated from herring sperm, between 5 and 8 hydrogen bonds can be ruptured reversibly before the molecule breaks down; spontaneously rendering it inactive. Therefore, a model for the thermal process consistent with this general behavior is one that assumes that a successive number of bonds need to be broken reversibly up to a point whereupon the reaction becomes irreversible and the macromolecule is inactivated. The kinetic constant for each bond breakage is essentially the same since the energetics of the bonds to broken are much the same (at least in a stochastic sense) assuming independent events. Using heat, the reversible reaction is highly dependent upon the state of water since bound water gives physical structure to the molecule thereby determining the restoration forces which return the bond to its original state.

Likewise a suitable kinetic model for a radiation sterilization process again appears to be a series of reaction steps. However, due to the nature of the radiation attack each step would be considered to be irreversible.

In a multistep reaction scheme, the kinetic parameters for the forward reaction steps may or may not include a multiplicative statistical constant. If one postulates that 'n' events must occur at 'n' specific sites, then the probability of any one of 'n' bonds breaking is proportional to the number of unreacted sites. On the other hand, if one supposes that 'n' events can occur at any of a very large number of sites, then each step of the reaction scheme will be approximately equal since there is no significant depletion of reactive sites.

Each step of the reverse reaction scheme always includes a statistical factor since the probability that an injured molecule will repair one of its injured sites is proportional to the number of injured sites.

Thus, the proposed reaction mechanism for a thermal process schematically is shown in Figure 1.24 where the parenthesized symbols underlined by a dashed line are the proportionality factors if depletion of reactive sites occurs. If no depletion occurs, then the same scheme can be used without the proportionality factors.

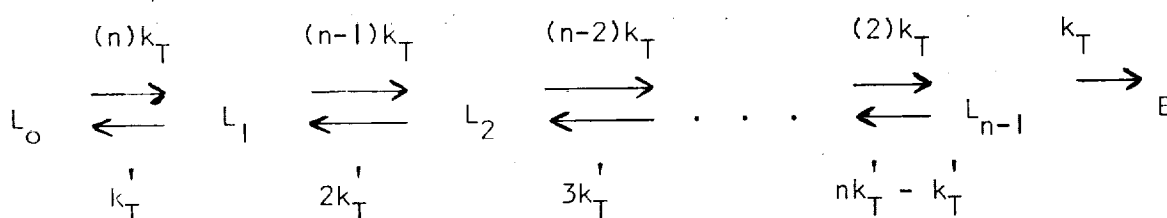


Figure 1.24: Reaction mechanism for thermal inactivation of microorganisms (Model Number 1)

Likewise for a radiation process the scheme would appear as shown in Figure 1.25 and the parenthesized symbols carry the same significance as above. In both sequences, L_i represents a viable spore which has 'i' injured sites and 'E' represents a dead spore.

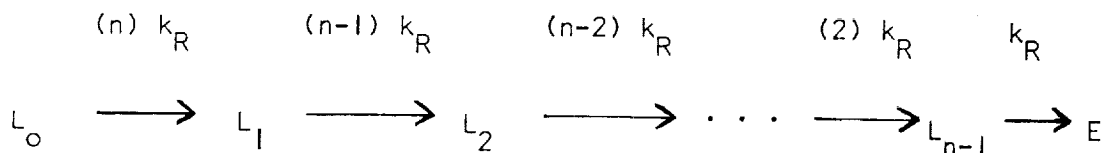


Figure 1.25: Reaction mechanism for radiation inactivation of microorganisms (Model Number 1)

When one starts to consider a thermoradiation process this reaction scheme takes on an expanded appearance. Death of the spore is still proposed to take place after a total of 'n' reaction steps. However, the 'n' steps can be completed with a number of combinations of either thermal or radiation steps. Schematically the thermoradiation process can be represented as shown in Figure 1.26, where L_{ij} represents a viable spore which has been thermally reacted at 'i' sites and injured at 'j' sites by radiation.

Details of each of the mechanistic schemes becomes apparent only after mathematical solution of the kinetic equations.

Mathematical Formulation

Characteristics of each of the kinetic mechanisms can be determined mathematically. The first step of such an analysis is to specify the relevant mathematical equations. For a thermal process the pertinent formulae result in the following system of linear, first order, ordinary differential equations:

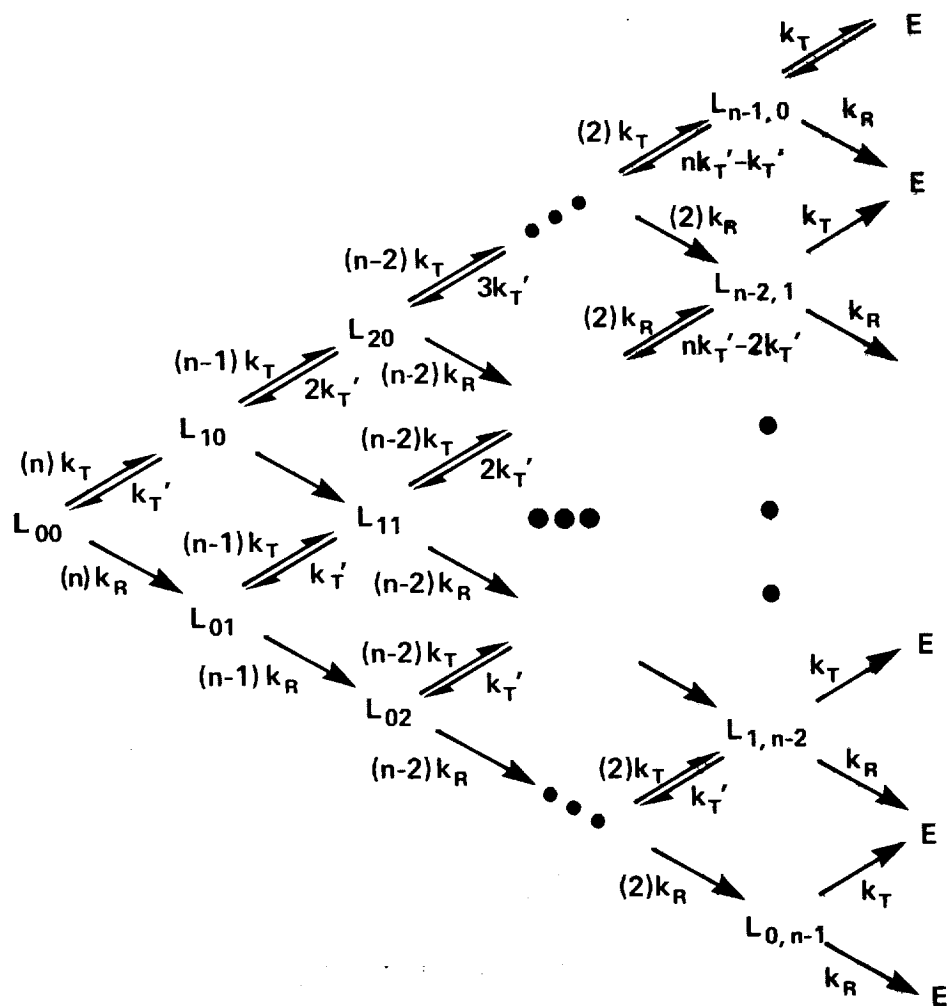


Figure 1.26: Reaction mechanism for thermoradiation inactivation of microorganisms (Model Number 1)

$$\frac{dL_0}{dt} = -(n)k_T L_0 + k_T^i L_1$$

$$\frac{dL_1}{dt} = (n)k_T L_0 - [(n-1)k_T + k_T^i] L_1 + 2k_T^i L_2$$

.

.

.

(1.2)

$$\frac{dL_{n-1}}{dt} = (2)k_T L_{n-2} - [nk_T^i - k_T^i + k_T] L_{n-1}$$

The mathematical system is uniquely determined once the initial condition is specified. The initial condition for this particular process is $L_0 = N_0$, $L_1 = L_2 = L_3 = \dots L_{n-1} = 0$ at $t = 0$. Again it should be noted that parenthesized symbols are to be used if we are considering the case of depletion of reactive sites; otherwise, they should be replaced by 1.0

This system of equations can be rewritten in matrix form.

$$\frac{d}{dt} \underset{\sim}{L} = \underset{\sim}{A} \underset{\sim}{L} \quad \text{and} \quad \underset{\sim}{L} = \underset{\sim}{L}^0 \text{ at } t = 0 \quad (1.3)$$

where $\underset{\sim}{L}$ and $\underset{\sim}{L}^0$ are the vectors:

$$\underset{\sim}{L} = \begin{pmatrix} L_0 \\ L_1 \\ L_2 \\ \vdots \\ L_{n-1} \end{pmatrix} \quad \text{and} \quad \underset{\sim}{L}^0 = \begin{pmatrix} N_0 \\ 0 \\ 0 \\ \vdots \\ 0 \end{pmatrix}$$

and A is a tridiagonal matrix of the form:

$$\underset{\sim}{A} = \begin{pmatrix} -(n)k_T & k_T^! & 0 & \dots & 0 \\ (n)k_T & -[(n-1)k_T + k_T^!] & 2k_T^! & & \vdots \\ 0 & (n-1)k_T & \cdot & \cdot & \vdots \\ \vdots & \cdot & \cdot & \cdot & nk_T^! - k_T^! \\ \vdots & \cdot & \cdot & \cdot & \vdots \\ 0 & \cdot & \cdot & \cdot & (2)k_T & -nk_T^! + k_T^! - k_T \end{pmatrix} \quad (1.4)$$

The mathematical system for radiological mechanisms has the same form except that no reversible reactions are present and therefore the matrix A does not have an upper diagonal.

For the proposed thermoradiation scheme, the mathematical system can again be represented in the matrix form. However, the matrix \tilde{A} is not as simply specified as it was in the thermal process due to the multiplicity of reaction routes. Equation 1.3 is still valid as long as \tilde{L} , \tilde{L}^0 and \tilde{A} are redefined as

$$\tilde{L} = \begin{pmatrix} L_{00} \\ L_{10} \\ L_{01} \\ L_{20} \\ L_{11} \\ L_{02} \\ \vdots \\ \vdots \\ L_{n-1,0} \\ \vdots \\ \vdots \\ L_{0,n-1} \end{pmatrix} \quad \tilde{L}^0 = \begin{pmatrix} N_0 \\ 0 \\ 0 \\ 0 \\ \cdot \\ \cdot \\ \cdot \\ 0 \end{pmatrix}$$

$$\tilde{A} = \begin{pmatrix}
 -(n)[k_T + k_R] & k_T^1 & 0 & 0 & 0 & 0 & \dots & 0 \\
 (n)k_T & -(n-1)[k_T + k_R] - k_T^1 & 0 & 2k_T^1 & 0 & 0 & & \\
 (n)k_R & 0 & -(n-1)[k_T + k_R] & 0 & k_T^1 & 0 & & \\
 0 & (n-1)k_T & 0 & -(n-2)[k_T + k_R] - 2k_T^1 & 0 & 0 & & \\
 0 & (n-1)k_R & (n-1)k_T & 0 & -(n-2)[k_T + k_R] - k_T^1 & 0 & & \\
 0 & 0 & (n-1)k_R & 0 & 0 & -(n-2)[k_T + k_R] & & \\
 \vdots & & & & & & \ddots & \\
 0 & \dots & & & & & & -[k_T + k_R]
 \end{pmatrix}$$

(1.5)

Vectors \tilde{L} and \tilde{L}^0 and matrix \tilde{A} have dimensions m where $m = n[n + 1]/2$.

(Equations 1.4 and 1.5 hold regardless of whether microorganisms are treated as chemical species which vary in a continuous fashion or are treated as discrete variables and must be treated as statistical variables.)

Mathematical Solutions

Unfortunately, these systems do not in general have explicit analytic solutions. Only the solution for the irreversible radiological mechanism can be expressed analytically.

If depletion of reactive sites is hypothesized then the fraction survival in a radiation mechanism scheme is

$$\frac{N}{N_0} = 1 - \left(1 - e^{-k_R t} \right)^n \quad (1.6)$$

where N = total number of survivors, both injured and uninjured. Equation 1.6 is the same expression as developed in Target Theory analysis by Powers (1962) and is also the same as the expression for clumps of 'n' microorganisms.

If depletion of reactive sites is not allowed, then the survival fraction is

$$\frac{N}{N_0} = e^{-k_R t} \sum_{r=0}^n \frac{(k_R t)^r}{r!} \quad (1.7)$$

The major difference between these two expressions is that when the survivor fraction is plotted in the normal semi-logarithmic fashion, the limiting slope of Equation 1.6 is $-nk_R$ whereas the limiting slope of Equation 1.7 goes to $-k_R$. Both forms show shoulders which become more prominent as 'n' grows large.

For the thermal and thermoradiation schemes, it is possible to solve the matrix equation and express the fraction survival in terms of matrix parameters. The solution for the matrix Equation 1.3 is

$$\tilde{L} = \sum_j \frac{\tilde{W}_j^T \tilde{L}^0}{\tilde{W}_j^T \tilde{Z}_j} \tilde{Z}_j e^{\lambda_j t} \quad (1.8)$$

where λ_j is the j th eigenvalue of the matrix \tilde{A}

\tilde{Z}_j is the j th eigenvector of the matrix \tilde{A}

\tilde{W}_j^T is the j th eigenrow of the matrix \tilde{A}

Thus the fraction survival is

$$\frac{N(t)}{N_0} = \sum_i \sum_j \frac{\tilde{W}_j^T \tilde{L}^0}{\tilde{W}_j^T \tilde{Z}_j} Z_{ij} e^{\lambda_j t} \quad (1.9)$$

where Z_{ij} is the i th element of the j th eigenvector.

Survival fractions have been calculated for each type mechanism for a representative number of kinetic parameters. All calculations were carried out numerically using a CDC 6600 computer located at the University of Minnesota Computer Center.

The salient features of each type of simulated process are described below.

Thermal Processes - For the thermal process represented in Figure 1.24, the fraction survival at time 't' depends on the number of reaction steps and the magnitude of the kinetic constants k_T and k_T' . Representative cases of simulated thermal processes are shown in Figures 1.27 and 1.28. Abscissa values are dimensionless values of $k_T t$.

Three important behavior patterns should be recognized. First, in Figure 1.27, as the number of events increases for a given set of values for k_T and k_T' , the slope of the survivor curve decreases. Although the value of 'n' is constant for death to be achieved, its value in this analysis is an undetermined adjustable constant.

The second noteworthy feature is the influence of the relative values of k_T and k_T' on the simulated D-value. In Figure 1.28, simulated survivor curves are shown computed using values of .5, 1, and 5 for k_T'/k_T . It is not surprising that larger values of k_T'/k_T should yield slower death responses; however, it is a mild surprise that when k_T'/k_T is increased five-fold from 1.0 to 5.0 that the D-value should increase by a factor as large as 16.

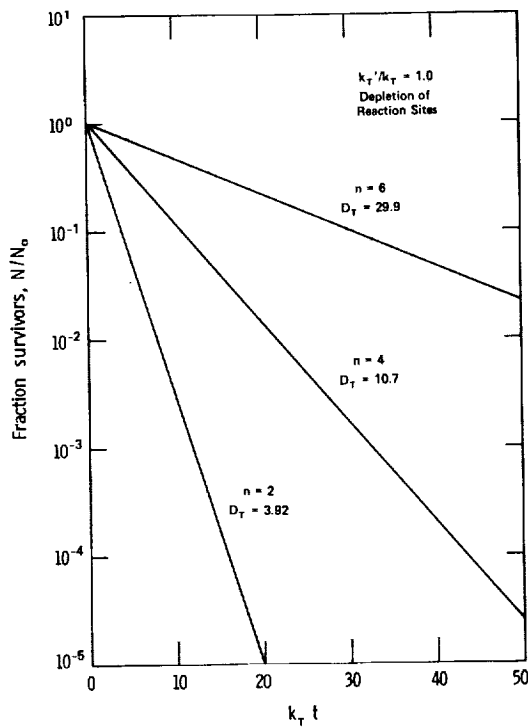


FIGURE 1.27: SIMULATED SURVIVOR CURVES SHOWING EFFECT OF INCREASING NUMBER OF REACTION STEPS BEFORE MICROORGANISM IS INACTIVATED.

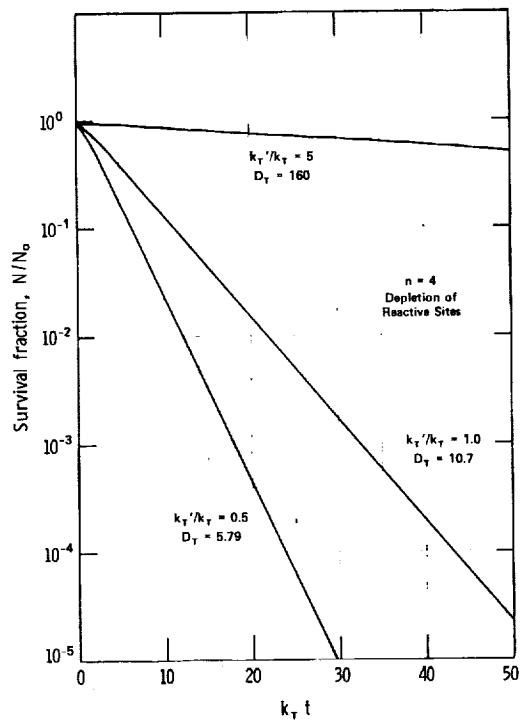


FIGURE 1.28: SIMULATED SURVIVOR CURVES SHOWING SYNERGISTIC BEHAVIOR EXHIBITED BY MODEL #1.

The significance of this result can be seen when studying dry heat sterilization in the following terms. It is not uncommon to find a fifty fold change in the D-value at a given temperature for a change in relative humidity from 20 to 100%. While bound water has always been recognized as influential in the survival ability of microorganisms, it has been difficult to characterize its role as one which could increase the integrity of a critical molecule by a factor of 50 using only relatively weak hydrogen bonding. On the other hand if such an increase was accomplished in a step-wise fashion the fifty fold change could be a by-product of a number of smaller increments and therefore would not be out of character.

Lastly, as k_T' is increased the survivor curves become more linear and lose the curvature most evident in the initial states of treatment - shown in Figure 1.28 for $k_T'/k_T = 0.5$. Recalling that lower values of relative humidity correspond to larger values of k_T' , a direct analogy can be drawn. Experimental survivor curves generated at high relative humidity generally have a concave downward curvature whereas survivor curves determined at moderate values of relative humidity are more apt to be linear. Thus the simulation of thermal processes responds in a manner parallel to a number of experimental responses. Unfortunately, the independent variables of the mathematical model can produce a given change in the simulated response in a number of ways. While the model can be fitted to the experimental data, the fit is somewhat arbitrary due to the multiplicity of sets of n , k_T and k_T' which could be used and is extremely dependent on small experimental variability.

Each of the curves in Figure 1.27 and Figure 1.28 was calculated assuming depletion of reactive sites. If one assumes that reactive sites are not depleted, the above observations and qualitative correlations are not significantly altered.

Radiation Processes - As previously mentioned, analytic solutions can be specified for the radiation reaction schemes. One generally supposes that the probability of occurrence of a radiological event is proportional to the energy dissipation of gamma radiation which in turn is proportional to gamma intensity. From Equations 1.6 and 1.7 one can see that if the kinetic constant for a given step is proportional to intensity, then the limiting over-all rate will likewise be proportional to intensity. (D-value will be inversely proportional.)

Data for radiation experiments are accurate enough that the model (Table 1.1) can be fitted to determine best fit values for the adjustable parameters n and k_R . Table 1.1 shows values for n and k_R which minimize the residue between experimental data and the theoretical function of Equation 1.6. Included in Table 1.1 are results for experiments in which spores were suspended in buffered solutions (originally reported in Progress Report #9) as well as for spores deposited on dry surfaces.

In all cases, the results indicate that the best fit is possible with multiple reaction steps. Slight variability in data accounts for the non-constancy of the determined value of n , although its value is always greater than 1.0. Variability of n in turn introduces a reflective change in the computed value of k .

TABLE 1.1: PARAMETERS FOR LEAST-SQUARES FIT OF TARGET THEORY MODEL
(EQU. 1.6) TO RADIATION EXPERIMENTAL DATA.

REGRESSION OF TARGET THEORY MATHEMATICAL MODEL
FOR RADIATION KINETICS

$$\frac{N(t)}{N_0} = 1 - (1 - \exp(-k_R t))^n$$

| Experiment Number | Values of n and k _R | | | | | |
|----------------------|--------------------------------|----------------|------------|----------------|-----------|----------------|
| | Dose Rate | | | | | |
| | 20 Krd/hr. | | 10 Krd/hr. | | 5 Krd/hr. | |
| | n | k _R | n | k _R | n | k _R |
| DF 2291 A-C (Wet) | 1.93 | 0.336 | 4.21 | 0.234 | 1.37 | 0.074 |
| DF 3106 A-C (Dry) | 1.94 | 0.553 | 1.78 | 0.323 | 3.79 | 0.231 |
| DF 3106 D-F (Dry) | 1.89 | 0.530 | 1.76 | 0.288 | 4.21 | 0.234 |
| DF 3142 A-C (Dry) | 1.99 | 0.526 | 1.75 | 0.295 | 5.03 | 0.236 |

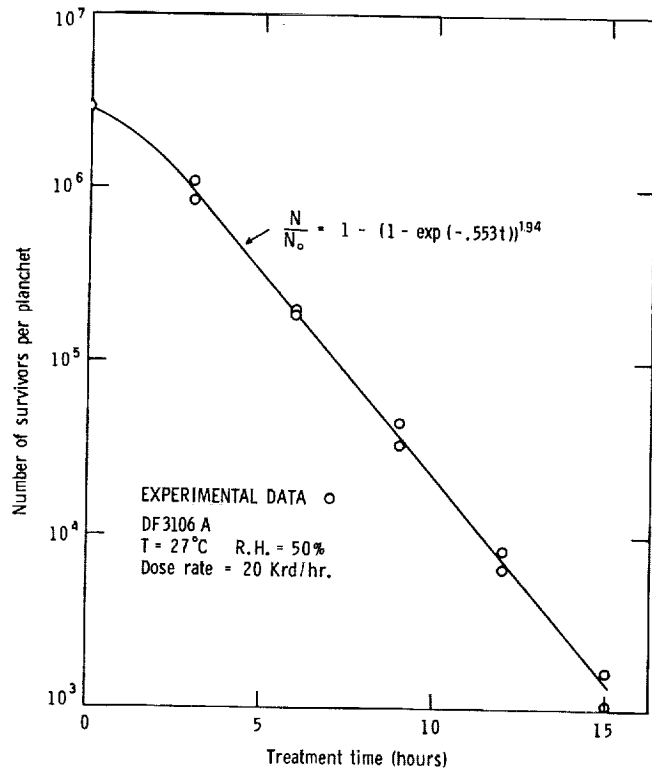


FIGURE 1.29: LEAST-SQUARES FIT OF TARGET THEORY MODEL TO
EXPERIMENTAL DATA OF RADIATION TREATMENT OF SPORES.

Figure 1.29 shows the match-up of the multi-step target theory model (Equation 1.6) to a set of experimental data.

The above results were once again computed assuming depletion of reactive sites. If one used Equation 1.7 under the assumption of no depletion of reactive sites, analysis would be limited to integral values of n , a restrictive condition.

Thermoradiation Processes - While thermal and radiological process simulations follow the general trends of their experimental counterparts, the model's value is much more evident when one simulates a thermoradiation process. Figure 1.30 shows the results of a simulation of a thermoradiation process along with the corresponding thermal and radiological simulations using realistic values for the kinetic parameters. Comparison shows that the model predicts a synergistic effect.

As in the thermal process simulation, experimental data can be fitted to the model by appropriate adjustments of the parameters n , k_T , k_T' and k_R . However, for the same reasons as before, such a fit carries little significance. It is not the object of this study to determine values for the independent variables of the model but rather to define and describe the source of the synergistic effect and its consequences on application of thermoradiation to microbiological systems.

To better achieve this goal, it is advantageous to define a performance parameter - Synergism Index (SI). This measure is used to quantify the amount of synergism in a given thermoradiation process.

Synergism index is therefore defined as:

Maximum synergism is in regions where thermal and radiation mechanisms are individually equally effective. Unfortunately only three radiation intensities were tested at each temperature and complete curves cannot be obtained from the limited amount of data. However, results do indicate a central tendency of SI relative to $D_T/D_{R0} = 1$.

In a similar fashion, data for dry-heat thermoradiation can be plotted. Unfortunately experimental noise factors combined with the fact that only three intensities were investigated at each psychrometric condition, individual bell-shaped curves could not be ascertained. When the composite results of all dry-heat experiments are plotted as shown in Figure 1.33 the central tendency and bell-shaped grouping can be seen. (Each point represents S.I. calculated using Equation 1.10 and geometric mean values for the necessary D-values.) Since these results were collected over a range of temperatures and a range of relative humidities, in a theoretical framework, they represent a range of values of k'_T/k_T , therefore a number of bell-shaped curves would need to be used to theoretically predict experimental patterns.

Conclusions and Extensions from Model Number 1

It should not be interpreted that the origin of the augmented death rate is the multitude of reaction routes per se. Rather, synergism arises by virtue of fewer reversible steps in thermal destruction routes once some of the injury stages have been reached using radiation. Reversibility is a necessary ingredient in this reaction scheme before synergism is evident. To illustrate this point, if two irreversible

Figure 1.29 shows the match-up of the multi-step target theory model (Equation 1.6) to a set of experimental data.

The above results were once again computed assuming depletion of reactive sites. If one used Equation 1.7 under the assumption of no depletion of reactive sites, analysis would be limited to integral values of n , a restrictive condition.

Thermoradiation Processes - While thermal and radiological process simulations follow the general trends of their experimental counterparts, the model's value is much more evident when one simulates a thermoradiation process. Figure 1.30 shows the results of a simulation of a thermoradiation process along with the corresponding thermal and radiological simulations using realistic values for the kinetic parameters. Comparison shows that the model predicts a synergistic effect.

As in the thermal process simulation, experimental data can be fitted to the model by appropriate adjustments of the parameters n , k_T , k_T' and k_R . However, for the same reasons as before, such a fit carries little significance. It is not the object of this study to determine values for the independent variables of the model but rather to define and describe the source of the synergistic effect and its consequences on application of thermoradiation to micro-biological systems.

To better achieve this goal, it is advantageous to define a performance parameter - Synergism Index (SI). This measure is used to quantify the amount of synergism in a given thermoradiation process.

Synergism index is therefore defined as:

$$SI = \frac{\text{Rate of a thermoradiation process}}{\text{Sum of the rates of the corresponding thermal and radiation processes}}$$

or mathematically expressed as:

$$SI = \frac{1/D_{TR}}{1/D_T + 1/D_{Ro}} \quad (1.10)$$

Thus, SI is the degree to which a thermoradiation reaction proceeds relative to the rates of the individual component reactions and therefore equals 1.0 if no synergism is apparent.

If one physical stress is dominant relative to the other, its effect dominates in a thermoradiation process and SI is near unity. In regions where the kinetics are not so dominated, synergism is an important consideration. The relative effectiveness of the independent stress will be used for parameterization purposes in terms of D_T/D_{Ro} .

Computed values of SI are shown in Figure 1.31 for simulations for four values of k_T'/k_T over the range of D_T/D_{Ro} . (Depletion of reaction sites and $n = 4$ have been assumed.) Thus, each curve corresponds to heat treatment at a given psychrometric condition while varying the radiation intensity. These results indicate that synergism reaches a maximal value in the region where thermal and radiological processes are equally effective. Also larger amounts of synergism appear to be possible as k_T'/k_T becomes large.

Experimental thermoradiation results can be plotted in similar fashion. Figure 1.32 shows values of SI calculated from wet-heat thermoradiation results. The points suggest a close family of curves with decreasing values of k_T'/k_T for increasing temperatures.

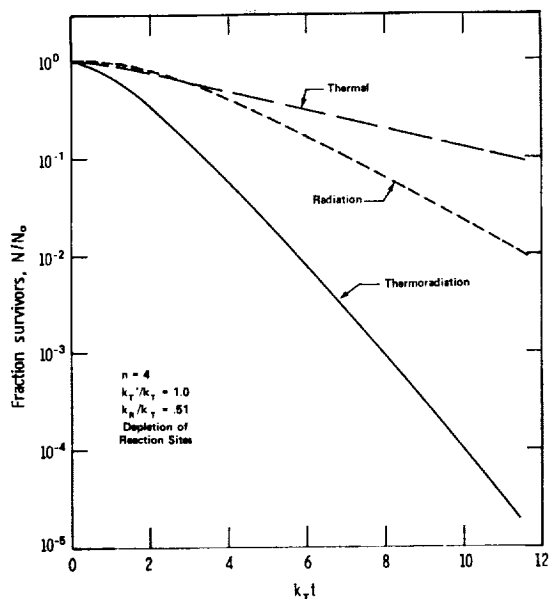


FIGURE 1.30: SIMULATED SURVIVOR CURVES SHOWING SYNERGISTIC BEHAVIOR EXHIBITED BY MODEL #1.

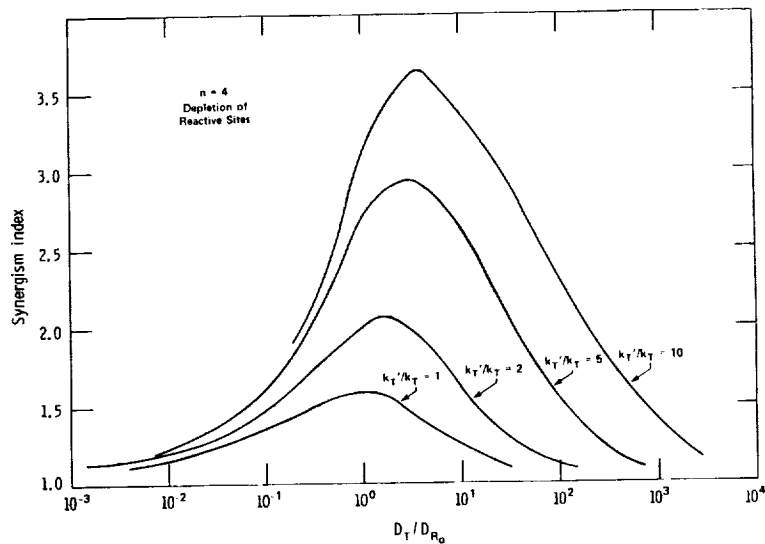


FIGURE 1.31: SYNERGISM INDEX OVER RANGE OF RADIOLOGICAL TREATMENT INTENSITIES RELATIVE TO THERMAL INACTIVATION RATES FOR VARIOUS VALUES OF k_T'/k_T .

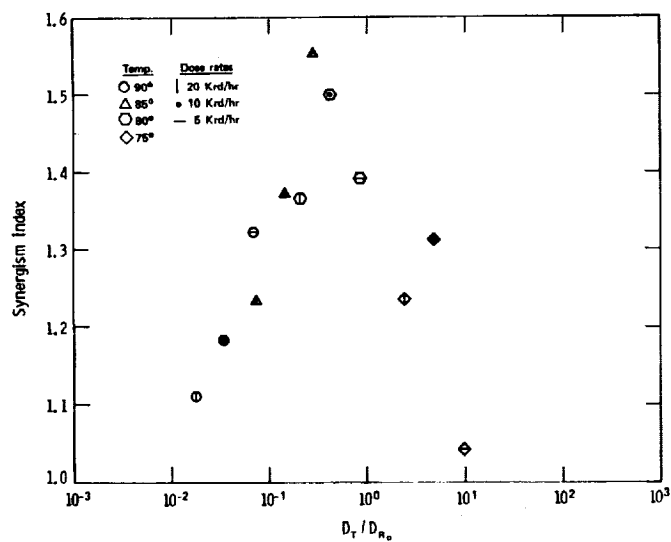


FIGURE 1.32: VALUES OF SYNERGISM INDEX CALCULATED FROM EXPERIMENTAL WET-HEAT THERMORADIATION STUDY.

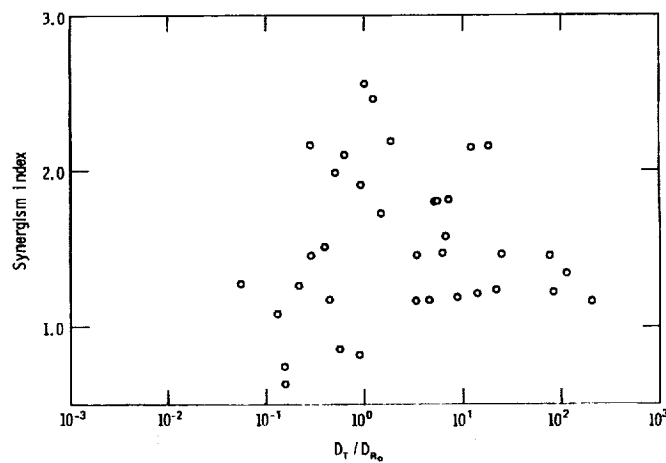


FIGURE 1.33: VALUES OF SYNERGISM INDEX CALCULATED FROM EXPERIMENTAL DRY-HEAT THERMORADIATION STUDY.

Maximum synergism is in regions where thermal and radiation mechanisms are individually equally effective. Unfortunately only three radiation intensities were tested at each temperature and complete curves cannot be obtained from the limited amount of data. However, results do indicate a central tendency of SI relative to $D_T/D_{R0} = 1$.

In a similar fashion, data for dry-heat thermoradiation can be plotted. Unfortunately experimental noise factors combined with the fact that only three intensities were investigated at each psychrometric condition, individual bell-shaped curves could not be ascertained. When the composite results of all dry-heat experiments are plotted as shown in Figure 1.33 the central tendency and bell-shaped grouping can be seen. (Each point represents S.I. calculated using Equation 1.10 and geometric mean values for the necessary D-values.) Since these results were collected over a range of temperatures and a range of relative humidities, in a theoretical framework, they represent a range of values of k_T'/k_T , therefore a number of bell-shaped curves would need to be used to theoretically predict experimental patterns.

Conclusions and Extensions from Model Number 1

It should not be interpreted that the origin of the augmented death rate is the multitude of reaction routes per se. Rather, synergism arises by virtue of fewer reversible steps in thermal destruction routes once some of the injury stages have been reached using radiation. Reversibility is a necessary ingredient in this reaction scheme before synergism is evident. To illustrate this point, if two irreversible

physical stresses are applied simultaneously to a multiple-step reaction series, (similar to scheme of Figure 1.26 but without reversible steps) then the viable fraction remaining at time t can be shown to be

$$\frac{N}{N_0} = 1 - \left(1 - \exp [- (k_1 + k_2) t] \right)^n \quad (1.11)$$

If depletion of reaction sites is assumed and

$$\frac{N}{N_0} = e^{-(k_1 + k_2)t} \sum_{r=0}^n \frac{[(k_1 + k_2)t]^r}{r!} \quad (1.12)$$

for no depletion. In these expressions, k_1 and k_2 are the kinetic constants for the individual mechanistic routes. Upon examination of Equation 1.11 and 1.12 relative to analogous expressions for the singular stress situations, no synergism is indicated.

Thus synergism can only be possible if one or both of the physical stresses produces reversible injury steps. If one wishes to project whether or not simultaneous application of two independent stresses will yield a synergistic response, the reversibility of injury steps must be known. For instance, combination of ethylene oxide (or other chemical sterilization agent) and gamma radiation would probably not show a synergistic response.

Model Number 2

A second model has also been conceived which holds many of the experimental features of thermoradiation. Similar to Model Number 1, the hypothesis of this model is that "death" is a result of a multi-event process. Thermal inactivation is viewed as basically a denaturation process while radiation is viewed as a degradation process where reaction occurs in the backbone of one chain of a critical double stranded macromolecule. "Death" is realized using radiation when both chains have been inactivated. Thermal processing leads to inactivation after a critical number of hydrogen bonds have been broken whereupon irreversible degradation of the molecule takes place.

Using both heat and radiation, the following sequence of events result in a synergistic effect to be observed: (1) one chain is severed by attack by radiation. (2) The molecule is more susceptible to thermal degradation at this injured system since each portion of the severed chain can be stripped from the companion strand more easily than can an uninjured chain. The denaturation process propagates from the dislocation site.

A convenient analogy can be drawn to the destruction of a zipper. A zipper can be broken by severing each side of the zipper (analogous to a radiation process), by pulling laterally on each side of the zipper until the zipper comes apart (analogous to thermally excited vibrations), or by cutting one side of the zipper and pulling laterally on the injured strand near the discontinuity.

This type of model conforms to the experimentally observed characteristics. First of all, the frequency of breaking one strand will be proportional to the intensity of radiation. Since the rate of creation of injured sites is the controlling step in this reaction scheme, the resulting synergism will be proportional to the intensity of radiation. Secondly, reaction route also depends on the relative humidity since the amount of bound water determines the resistance of the zipper to lateral stress and therefore the ability of the molecule to resist denaturation once injured. The hydrogen bonding of the water is analogous to the zipper cross linking.

Unfortunately, to set up a mathematical model, one needs to first formulate a physical model for the denaturation process featuring the resistance of a severed molecule to torsional strain and the influence of bound water on this resistance. The hypothesis upon which such a model would be based is extremely tenuous and the corresponding mathematical model would likewise be terribly tentative. Therefore, further characterization of this model is beyond the scope of this research effort and we have to be satisfied with only a qualitative analysis.

CONCLUSIONS

1. Dry-heat thermoradiation experiments show a synergistic effect, the degree of which depends on radiation intensity, temperature, and relative humidity.
2. A physical and mathematical model has been derived which first of all predicts a synergistic effect and secondly displays a priori many of the salient features experimentally observed. This model is useful for the execution of further thermoradiation experiments and relates to future testing for synergistic effects between other combinations of physical stresses.

REFERENCES

- Cox, R. A., and Peacocke, A. R.: 1957. Denaturation Theory: Cooperative Breakage of Hydrogen Bonds. J. Poly. Sci., vol. 23, pp. 765-779.
- Powers, E. L.: 1967. Considerations of Survival Curves and Target Theory. Physics in Medicine and Biology, vol. 7, pp.3-28.
- Webb, R. G., Ehret, C. F., and Powers, E. L.: 1958. A Study of The Temperature Dependence of Radiation Sensitivity of Dry Spores of Bacillus Magaterium between 5°K and 309°K. Experientia, vol. 14, pp. 324-326.

